

AEROSPACE REPORT NO.
ATR-76(7911)-2

EQUIPMENT SYSTEMS IMPROVEMENT PROGRAM

FINAL REPORT

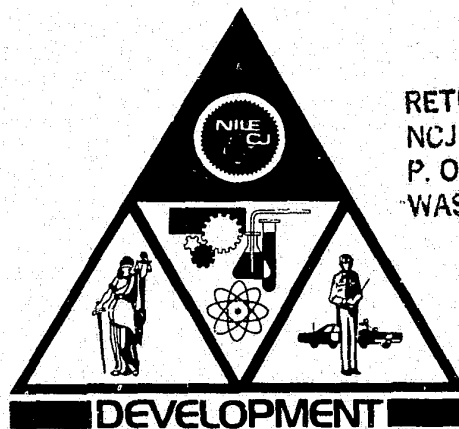
**AN INVESTIGATION OF THE FEASIBILITY
OF THE USE OF THE LASER OPTOACOUSTIC
TECHNIQUE FOR THE DETECTION OF EXPLOSIVES**

Law Enforcement Development Group

May 1976

LOAN DOCUMENT

RETURN TO:
NCJRS
P. O. BOX 24036 S. W. POST OFFICE
WASHINGTON, D.C. 20024



C.3

35583

Prepared for

**National Institute of Law Enforcement and Criminal Justice
LAW ENFORCEMENT ASSISTANCE ADMINISTRATION
U.S. DEPARTMENT OF JUSTICE**

The Aerospace Corporation

LOAN DOCUMENT

RETURN TO:
NCJRS
P. O. BOX 24036 S. W. POST OFFICE
WASHINGTON, D.C. 20024

Aerospace Report No.
ATR-76(7911)-2

EQUIPMENT SYSTEMS IMPROVEMENT PROGRAM

FINAL REPORT

AN INVESTIGATION OF THE FEASIBILITY OF THE USE
OF LASER OPTOACOUSTIC DETECTION FOR THE
DETECTION OF EXPLOSIVES

NCJRS

AUG 4 1976

Prepared by

Case Western Reserve University
Cleveland, Ohio 44106

ACQUISITIONS

Under Subcontract 44343-V to
Law Enforcement Development Group
THE AEROSPACE CORPORATION
Washington, D. C. 20024

May 1976

Prepared for

National Institute of Law Enforcement
and Criminal Justice
LAW ENFORCEMENT ASSISTANCE ADMINISTRATION
U. S. DEPARTMENT OF JUSTICE

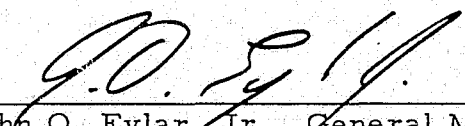
Contract No. J-LEAA-025-73

This project was supported by Contract Number J-LEAA-025-73 awarded by the National Institute of Law Enforcement and Criminal Justice, Law Enforcement Assistance Administration, U.S. Department of Justice, under the Omnibus Crime Control and Safe Streets Act of 1968, as amended. Points of view or opinions stated in this document are those of the authors and do not necessarily represent the official position or policies of the U.S. Department of Justice.

EQUIPMENT SYSTEMS IMPROVEMENT PROGRAM

AN INVESTIGATION OF THE FEASIBILITY OF THE USE
OF THE LASER OPTOACOUSTIC TECHNIQUE FOR THE
DETECTION OF EXPLOSIVES

Approved



John O. Eylar, Jr., General Manager
Law Enforcement and Tele-
communications Division

ABSTRACT

A study has been carried out to explore the feasibility of detecting various explosive vapors in the presence of known interferences, using the technique of laser optoacoustics. Measurements were made in the 6, 9, and 11 micrometer regions. In the 6 micrometer region, strong interference by water vapor made the sensitive detection of explosives vapors infeasible. In the 9 and 11 micrometer regions, interferences were substantially reduced, and the explosive vapors ethylene glycol dinitrate, nitroglycerine, and 2 to 4 dinitrotoluene could be sensitively detected. Additional measurements are recommended to verify that the technique has practical feasibility.

CONTENTS

ABSTRACT	v
PREFACE	xiii
SUMMARY	xv
I. INTRODUCTION	1
II. SUMMARY OF PRINCIPAL RESULTS	3
III. FEASIBILITY INVESTIGATIONS	5
A. Basic Component Investigation	5
B. Investigation of Interfering Species	37
C. Determination of Optoacoustic Spectra of Explosives Vapor in the Presence of Interfering Species	37
IV. FEASIBILITY DETERMINATIONS	41
A. Optoacoustic Efficiency	41
B. Interference	43
C. System Design Considerations	45
V. RECOMMENDATIONS	51
APPENDIX A: A RATE EQUATION DESCRIPTION OF A TWO-LEVEL OPTOACOUSTIC SYSTEM	53
APPENDIX B: COLLECTION OF OPTOACOUSTIC SPECTRA OF EXPLOSIVES AND INTERFERENCES TAKEN AT 6 μm (CO LASER) AND 9 AND 11 μm (CO ₂ LASER)	61
NOTES	91

FIGURES

1.	Molecular Processes in Optoacoustic Spectroscopy	6
2.	Variation of Optoacoustic Signal with Incident Power	9
3.	Block Diagram of Apparatus Used in Study	10
4.	Optoacoustic Equipment Used in the Laboratory	14
5.	Optoacoustic Equipment Used in Field Trial	14
6.	Frequency Response of the Optoacoustic Cell	15
7.	Drawing of the Optoacoustic Cell	18
8.	Test for Linearity Using 20 CO ₂ Laser Lines	22
9.	Schematic Representation of Spectral Distribution of Absorptions of Explosives and Interfering Species	31
10.	Vapor Pressure of Explosives	32
B-1.	Optoacoustic Spectrum of NG at 6 Micrometers (45°C)	63
B-2.	Optoacoustic Spectrum of EGDN (10% NG) at 6 Micrometers (45°C)	64
B-3.	Optoacoustic Spectrum of DNT at 6 Micrometers (45°C)	65
B-4.	Optoacoustic Spectrum of TNT at 6 Micrometers (45°C)	66
B-5.	Optoacoustic Spectrum of RDX at 6 Micrometers (45°C)	67
B-6.	Optoacoustic Spectrum of PETN at 6 Micrometers (45°C)	68
B-7.	Optoacoustic Spectrum of TOVEX at 6 Micrometers (45°C)	69
B-8.	Optoacoustic Spectrum of Dynamite at 6 Micrometers (45°C)	70

FIGURES (Continued)

B-9.	Optoacoustic Spectrum of NG at 9 Micrometers (45°C)	71
B-10.	Optoacoustic Spectrum of EGDN at 9 Micrometers (45°C)	72
B-11.	Optoacoustic Spectrum of DNT at 9 Micrometers (45°C)	73
B-12.	Optoacoustic Spectrum of Dynamite at 9 Micrometers (45°C)	74
B-13.	Optoacoustic Spectrum of Black Powder at 9 Micrometers (45°C)	75
B-14.	Optoacoustic Spectrum of NG at 11 Micrometers (23°C)	76
B-15.	Optoacoustic Spectrum of NG at 11 Micrometers (45°C)	77
B-16.	Optoacoustic Spectrum of EGDN at 11 Micrometers (23°C).	78
B-17.	Optoacoustic Spectrum of EGDN at 11 Micrometers (45°C).	79
B-18.	Optoacoustic Spectrum of Butane at 6 Micrometers	80
B-19.	Optoacoustic Spectrum of Methane at 6 Micrometers	81
B-20.	Optoacoustic Spectrum of NO at 6 Micrometers	82
B-21.	Optoacoustic Signal of NO ₂ at 6 Micrometers	83
B-22.	Optoacoustic Spectrum of Water Vapor at 6 Micrometers.	84
B-23.	Optoacoustic Spectrum of Butane at 9 Micrometers	85
B-24.	Comparison of EGDN and Water Vapor Optoacoustic Spectra at 6 Micrometers (50% Relative Humidity)	86
B-25.	Comparison of NG and Water Vapor Optoacoustic Spectra at 6 Micrometers (20% Relative Humidity)	87

FIGURES (Continued)

B-26. Comparison of NG and Water Vapor Optoacoustic Spectra at 6 Micrometers (50% Relative Humidity)	88
B-27. Optoacoustic Detection of SF ₆ in the 10.6 Micrometer Wavelength Region	89

TABLES

1.	Laser Wavelengths Used in Optoacoustic Investigation	12
2.	Minimum Detectable Explosive Concentration Using Four Wavelengths	24
3.	Analysis of Reproducibility of Data - NG and Air, 50 Milliwatts Power	29
4.	Explosive Optoacoustic Spectra (Microvolt per Milliwatt) in the 6 Micrometer Region	34
5.	Explosive Optoacoustic Spectra (Microvolt per Milliwatt) in the 9 Micrometer Region	35
6.	Explosive Optoacoustic Spectra (Microvolt per Milliwatt) in the 11 Micrometer Region	36
7.	Concentration of Interfering Species (partial pressure) in Nitrogen	38
8.	Pollutant Optoacoustic Spectra (Microvolt per Milliwatt) in the 6 Micrometer Region	39
9.	Optoacoustic Efficiency of Explosives and Interfering Species at 6 Micrometers	42

PREFACE

This document represents the final report of a subcontract effort by the Case Western Reserve University on the feasibility of the laser optoacoustic technique for explosives vapors detection.

The original Case Western report (submitted in April 1975) was reviewed by a number of qualified agencies, as well as The Aerospace Corporation and the National Institute of Law Enforcement and Criminal Justice. As a result of those reviews, additional technical material was requested of, and submitted by, Case Western in an addendum letter. The addendum results have been integrated into the final report by The Aerospace Corporation. The entire report has been edited and retyped by The Aerospace Corporation for typographical errors and standardization.

It is emphasized that the technical contents of this document are Case Western data and evaluations under the subcontract. No new data have been generated or included since that subcontract was completed. The recommendations in Chapter V are those of Case Western Reserve. Concurrence by The Aerospace Corporation is neither stated nor implied.

Some technical notes have been incorporated into the text where appropriate. As an example, many of the optoacoustic spectra for explosives may be contaminated with water vapor. Later vapor characterization work on PETN and RDX has shown almost negligible vapor pressure for these explosives; therefore, the absorption lines indicated in Figures B-3 and B-4 are believed to be essentially those of water.

SUMMARY

The ability to detect small quantities of explosives in relatively large volumes may require the development and refinement of techniques not presently in commercial use. This report documents the work performed in probing one of these techniques: laser optoacoustics.

Optoacoustics itself is not a new technique but has received increased attention with the advent of tunable lasers. A laser beam is focused into a cell containing a gas sample of interest. If certain gas sample constituents absorb this radiation, the gas will heat up, thereby producing an increase in pressure which can be detected by a sensitive microphone.

This technique appeared to have a minimum detection limit and a sufficient potential for improved specificity in comparison to available vapor detectors to warrant a detailed investigation. The Aerospace Corporation, under contract to the Law Enforcement Assistance Administration, awarded a subcontract to the Case Western Reserve University to investigate the feasibility of the laser optoacoustic technique for the detection of explosives vapors. The purpose of the subcontract was to measure the strengths of laser optoacoustic signals for common explosives and selected interference gases to determine whether explosive signals of interest could be detected in the presence of interferences. The infrared spectral region most conducive to good detection was also to be determined.

Case Western Reserve University utilizing both carbon dioxide and carbon monoxide lasers scanned thirty-nine wavelengths in the 6, 9, and 11

micrometer spectral regions of the infrared. Nine explosives were investigated at a variety of available wavelengths. The explosives examined were:

Nitroglycerine

Ethylene Glycol Dinitrate

Dinitrotoluene

Trinitrotoluene

RDX

PETN

Tovex

Dynamite

Black Powder

Several other gases were also examined which may act as interferences to the detection of explosives.

The results of the study indicate that although explosives exhibit significant absorption in the 6 micrometer region, the strong absorption by water in this region precludes the detection of explosives vapors at the required lower concentration. Further work indicated that water does not absorb as strongly in the 9 to 11 micrometer region and that a number of explosive vapors did exhibit significant absorption in this region.

Although not all of the explosives and potential interferences could be checked for absorption at all of the longer wavelengths, it was concluded that a field operable instrument probably could be developed using the longer wavelength region for operation. However, a more thorough study of explosives and interference absorptions in the 9 to 11 micrometer regions would be required before prototype development should be begun.

CHAPTER I. INTRODUCTION

The objective of this study was to determine the feasibility of using a laser optoacoustic device to detect the presence of minute quantities of trace vapors emitted by various explosives. The motivation for the study is the need for a method of detecting the presence of explosives without extensive search and without disturbance of the explosives. An effective detection method would be a great deterrent to both illegal and unauthorized use of explosives.

One means of detecting explosives is by detecting the vapors they emit. These vapors can be identified by various chemical and physical properties of the constituent molecules.

The optoacoustic method is not new. It has been known for years that it is possible to focus modulated radiation into an absorbing gas, causing it to heat up slightly and thereby generate a pressure wave inside the gas vessel. The pressure wave can be detected with a sensitive microphone. This type of system is used in industry either to monitor the presence of the gas or the level of the incident radiation. This method is particularly sensitive if the incident radiation is strongly absorbed by the gas. The optoacoustic method took on new dimensions with the advent of tunable lasers. With lasers, the method is not only sensitive but can be specific for molecular species that exhibit unique optoacoustic signatures as the laser is tuned over ten or more appropriate wavelengths.

A summary of the principal results is presented in Chapter II of this report. Details of equipment, experimental methods, and results are presented in Chapter III. The significance of these results is discussed in Chapter IV, and recommendations for further action are presented in Chapter V.

CHAPTER II. SUMMARY OF PRINCIPAL RESULTS

This investigation into the feasibility of using a laser optoacoustic device to detect explosives vapors resulted in the following significant findings:

- a. In the absence of interfering species, nitroglycerine (NG), ethylene glycol dinitrate (EGDN) and dinitrotoluene (DNT) can be unmistakably detected in the 6 micrometer, 9 micrometer and 11 micrometer wavelength regions.
- b. Interfering species are either environmental or are associated with the explosive itself or its containment. Atmospheric "pollutants" such as nitric oxide (NO), nitrogen dioxide (NO₂), methane (CH₄), water vapor, isobutane and normal butane are examples of the first category; nitrobenzene, alcohol, cyclohexanone, and xylene are examples of the latter.

In the 6 micrometer wavelength region [carbon monoxide (CO) laser], both NO₂ and water vapor cause troublesome interference. In the 9.8 to 11 micrometer wavelength region, butane vapors are troublesome. The 6 micrometer wavelength region should perhaps be avoided in favor of the 9.2 to 9.7 micrometer and the 11 to 12 micrometer wavelength regions, where there is substantially less interference from water vapor. Radiation at these wavelength regions is available from mixed isotope carbon dioxide (CO₂) lasers, such as those used in the present investigation.

- c. The presence of SF_6 vapor emitted by a simulated blasting cap and by pieces of Teflon impregnated with SF_6 over a year earlier was readily detected with an optoacoustic detector using radiation in the 10.6 micrometer wavelength region. In these favorable circumstances, the signals were so strong that neither environmental nor sample-related interfering species caused significant interference. More specifically, the peak values of the optoacoustic signals were 714 microvolts per milliwatt ($\mu V/mW$) and 4 $\mu V/mW$ for the blasting cap and the Teflon capsules, respectively. The strongest interfering signal was of the order of $\leq 0.5 \mu V/mW$, resulting in a signal-to-noise ratio of at least eight.
- d. A portable, field operable, long-lived laser optoacoustic detector can be implemented; however, the feasibility of detecting the low levels of characteristic vapors from explosives in the presence of interference must be firmly established before such a development is initiated.

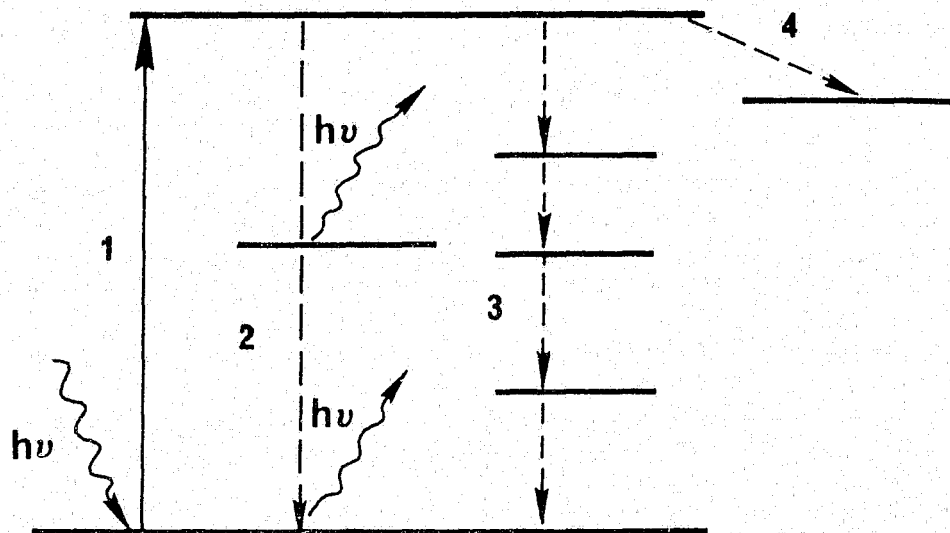
Preliminary estimates indicate that power consumption in the operating mode can be less than 200 watts, overall weight can be less than 100 pounds (separable into two or three component parts of less than 40 pounds each, with dimensions comparable to those of small suitcases or backpacks used by hikers).

CHAPTER III. FEASIBILITY INVESTIGATION

A. Basic Component Investigation

1. Optoacoustic detection method: underlying principles and experimental techniques. In the context of the present investigation, the presence of minute quantities of explosives vapor in a "carrier" gas, such as air or nitrogen, is detected by exposing the gas mixture to monochromatic infrared radiation. This incident radiation is absorbed by the explosives molecules, which store the energy internally in the form of vibrational energy. Non-resonant collisions with carrier gas molecules result in transfer of the internal vibrational energy (in the explosives molecules) to the molecules of the carrier gas, in the form of external translational energy. This energy becomes manifest in the form of minute increases in temperature. An increase in pressure occurs if the gas is contained in a closed cell. If the incident radiation is modulated, sound waves are produced inside the gas container and these can be detected with very sensitive microphones.

The two basic molecular processes just described and two other competing processes are illustrated schematically in Figure 1. Absorption is illustrated as Process 1 and vibrational-translational (V-T) energy transfer is shown as Process 3. In the present context, the magnitude of the optoacoustic signal can be significantly decreased by the competing effects of Processes (2) and (4). In Process (2), the excited state decays through



Legend:

1. Incident radiation absorbed in an allowed molecule undergoes vibrational-rotational excitation
2. Fluorescence decay through a number of allowed transitions; several photons emitted
3. Vibrational-translational energy transfer; many intermediate energy levels usually involved
4. Internal energy trapping in a state not accessible to vibrational-translational energy transfer

Figure 1. Molecular Processes in Optoacoustic Spectroscopy

spontaneous emission, whereas in Process (4), vibrational energy is trapped internally and degraded from one vibrational mode into another, until all phase relationship with the modulation reference signal is lost.

In the interest of completeness, a simple rate equation description of the optoacoustic process is provided in Appendix A. Equation (A-9) of that account yields the result that the magnitude of the optoacoustic signal is proportional to

$$\frac{1}{2} \frac{\tau_c^{-2} B N I_o}{(B I_o + \tau_c^{-1})^2}$$

where

N = number density of explosives vapor given in molecules per cubic centimeter (cm^3)

I_o = intensity of incident radiation per unit time given in watts per square centimeter second ($\text{W}/\text{cm}^2\text{-sec}$)

B = Einstein coefficient for stimulated absorption and emission,

$$\tau_c^{-1} = \tau_c^{-1} + \tau_R^{-1}$$

τ_c^{-1} = rate of de-excitation due to collisions

τ_R^{-1} = radiative rate of de-excitation due to fluorescence decay

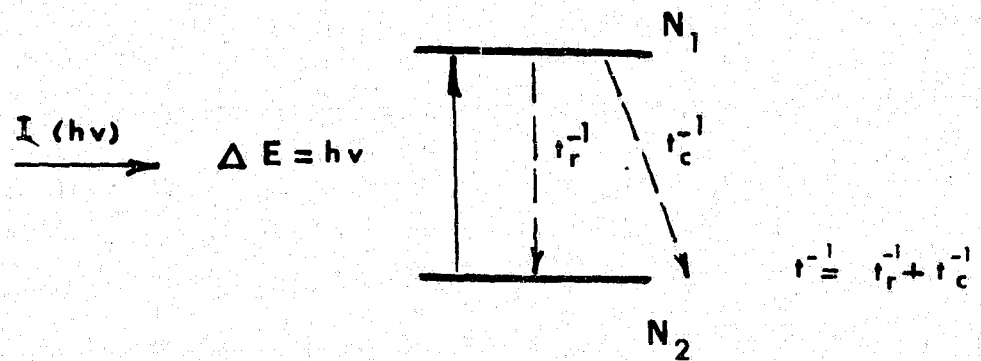
This result indicates that optimum conditions are attained when $B I_o = \tau_c^{-1}$. Since, in practice, near standard conditions, τ_R^{-1} is not likely to be larger than 10^5 whereas τ_c^{-1} is not likely to be less than 10^6 , then for optimum conditions $B I_o \cong \tau_c^{-1}$; this means that it is not useful to excite

molecules at a rate higher than they can be de-excited by vibrational-translational transfer. In fact, if BI_0 exceeds τ^{-1} greatly, the signal actually starts to decrease as $1/I_0$. These considerations are illustrated schematically in Figure 2. Indicated also is the fact that, for a variety of reasons, there is also an initial dead zone, and no optoacoustic signal is detected for power levels below threshold.

A block diagram of the apparatus used in this investigation is shown in Figure 3.

Two types of lasers, CO and CO₂, were used to measure the optoacoustic spectra of the explosives. The CO laser was a sealed-off, dry ice cooled, grating tuned device using ¹²C¹⁶O as the lasing gas. This laser could be tuned from well below 5.8 micrometers to above 6.6 micrometers, with output power ranging from a few hundred milliwatts at the shorter wavelengths to about 70 milliwatts at 6.6 micrometers.* The 15 wavelengths

*It was initially felt that to achieve single line operation at wavelengths greater than 6 micrometers it would be necessary to use ¹³C¹⁸O as the lasing gas. After considerable effort, it was discovered that whereas ¹²C¹⁶O could be operated satisfactorily in the sealed-off mode, ¹³C¹⁸O, as supplied, contained impurities in significant quantities, and sealed-off operation with it could not be sustained. Moreover, the high cost of ¹³C¹⁸O prohibits flowing operation. Fortunately at about that time, operating techniques had been sufficiently developed so that significant single line power could be obtained with ¹²C¹⁶O up to 6.626 micrometers. Further increases in wavelength being of no interest, efforts to use ¹³C¹⁸O were discontinued.



OPTOACOUSTIC SIGNAL $\propto \frac{BNI\tau_c^{-1}}{2(BI + \tau^{-1})^2}$

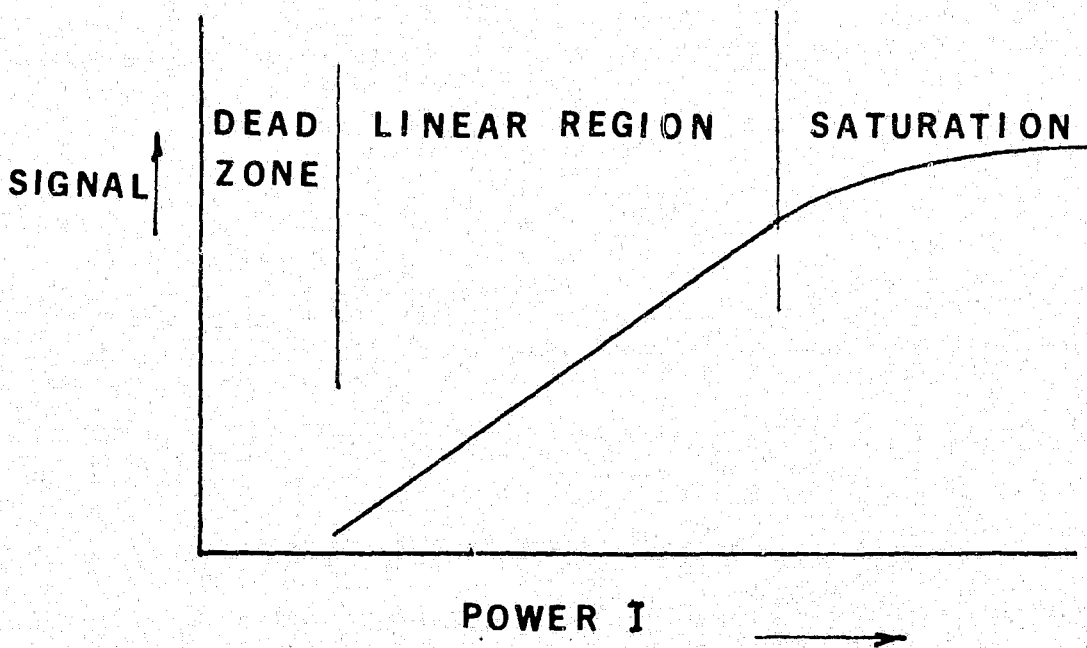


Figure 2. Variation of Optoacoustic Signal With Incident Power

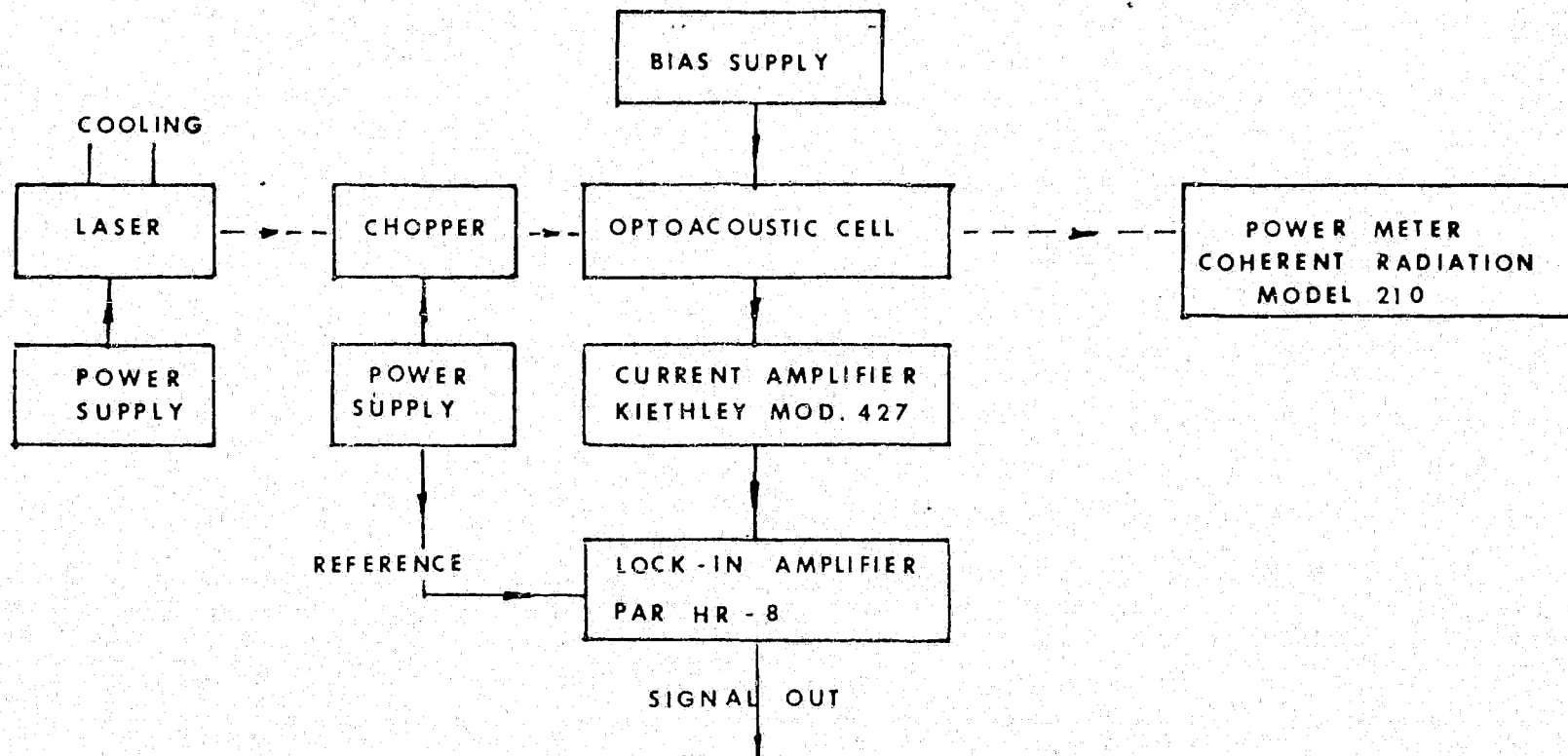


Figure 3. Block Diagram of Apparatus Used in Study

used in the $^{12}\text{C}^{16}\text{O}$ laser part of the study spanned the region from 5.837 to 6.626 micrometers; they are listed in Table 1.

Excitation in the 9 micrometer and 11 micrometer regions was obtained by using two CO_2 lasers. In the 9 micrometer region, the device was a flowing gas, water cooled, grating tuned laser using $^{12}\text{C}^{16}\text{O}_2$ as the active medium. Fourteen wavelengths, ranging from 9.217 to 9.711 micrometers, with powers to 1 watt, were used in this region. These are also listed in Table 1.

In the 11 micrometer region, a sealed-off, water cooled, grating tuned laser containing a mixture of $^{12}\text{C}^{16}\text{O}_2$ and $^{13}\text{C}^{16}\text{O}_2$ was used for excitation. The nine wavelengths, spanning the region from 10.753 to 11.194 micrometers, that were used in this part of the study are also listed in Table 1.

The optoacoustic detector used for this work is a high sensitivity device. Sodium chloride (NaCl) windows are used to permit entrance and exit of the exciting radiation. The cell is capable of being evacuated to a moderate vacuum (~ 1 Torr) to enable rapid and positive removal of vapors between sample runs. Heater coils are provided to permit operation at elevated temperatures. The detectivity of the cell was measured by using SF_6 excited with 10.571 micrometer radiation. The cell was shown to detect one part in 10^6 SF_6 in air with a signal-to-noise ratio of 10^5 , indicating an extrapolated sensitivity of one part in 10^{11} (vapor phase), assuming a signal-to-noise ratio of unity. A view of the apparatus used in the laboratory

Table 1. Laser Wavelengths Used in Optoacoustic Investigation

$^{12}\text{C}^{16}\text{O}$		$^{12}\text{C}^{16}\text{O}_2$		$^{13}\text{C}^{16}\text{O}_2$	
<u>Wavelength (Micrometers)</u>	<u>Max Power Available (Milliwatts)</u>	<u>Wavelength (Micrometers)</u>	<u>Max Power Available (Watts)</u>	<u>Wavelength (Micrometers)</u>	<u>Max Power Available (Watts)</u>
5.837	400	9.217	1.2	10.753	1.6
5.880	190	9.247	2.6	10.783	1.9
5.941	215	9.280	3.7	10.800	1.9
6.002	250	9.303	4.3	10.833	1.5
6.063	200	9.352	3.7	10.850	-
6.132	175	9.455	-	11.065	1.3
6.174	110	9.486	3.2	11.107	1.9
6.213	145	9.501	-	11.149	1.8
6.258	200	9.550	-	11.194	1.4
6.312	110	9.584	4.0		
6.367	135	9.601	3.8		
6.408	80	9.655	-		
6.465	90	9.673	2.4		
6.538	50	9.711	1.0		
6.602	20				
6.626	40				

investigations is shown in Figure 4 and a view of the field operable unit is provided in Figure 5.

The exciting radiation was chopped with a variable rate mechanical chopper, and all signal measurements were made by using standard phase-sensitive techniques with reference to the chopping frequency. Signal amplification and detection was accomplished with a Keithley Instruments Model 427 Current Amplifier and a PAR Model HR-8 Lock-In Amplifier. Laser power measurements were made with a Coherent Radiation Model 210 Power Meter.

In most instances, the cell was evacuated with the explosives sample in place, after which the cell was filled with dry nitrogen, or with air, or with air containing some interfering species. In all measurements, since a closed system was used, it was assumed that the explosives vapors were at thermal equilibrium with the source.

Details of the laboratory system and concepts follow:

a. Optoacoustic Cell

1. Frequency Response

Optoacoustic response vs. chopping frequency is shown in Figure 6.

2. Sensitivity Determination

The sensitivity of the optoacoustic cell has been determined for SF₆ at 10.571 micrometers, the wavelength of the P(18) line

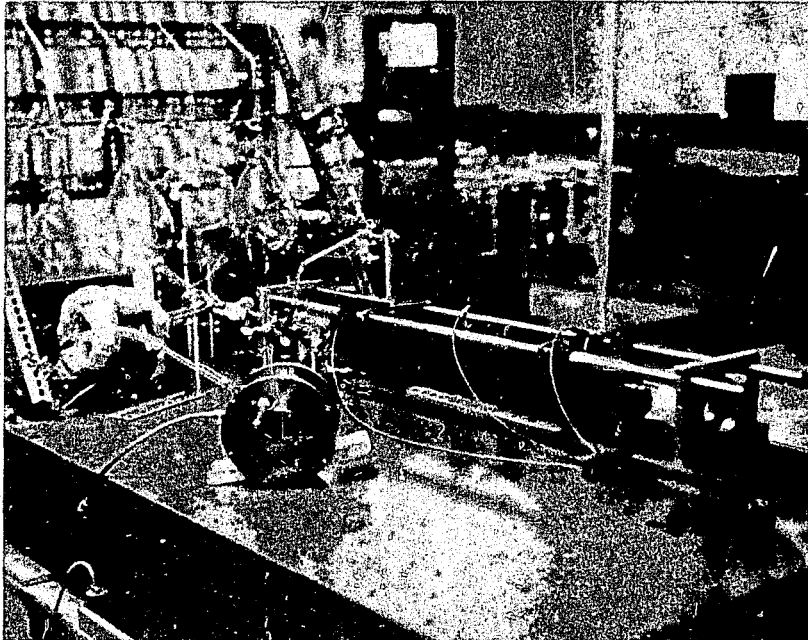


Figure 4. Optoacoustic Equipment Used in the Laboratory

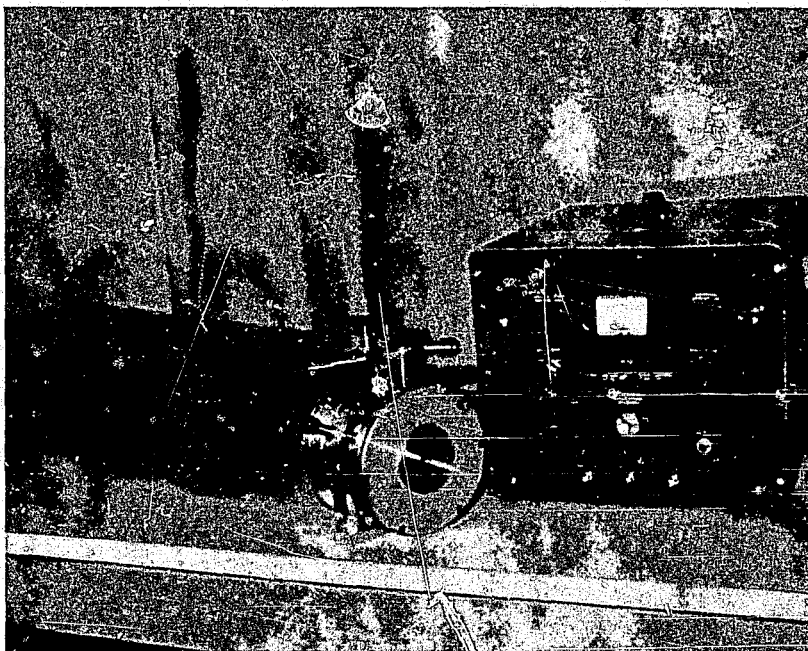


Figure 5. Optoacoustic Equipment Used in Field Trial

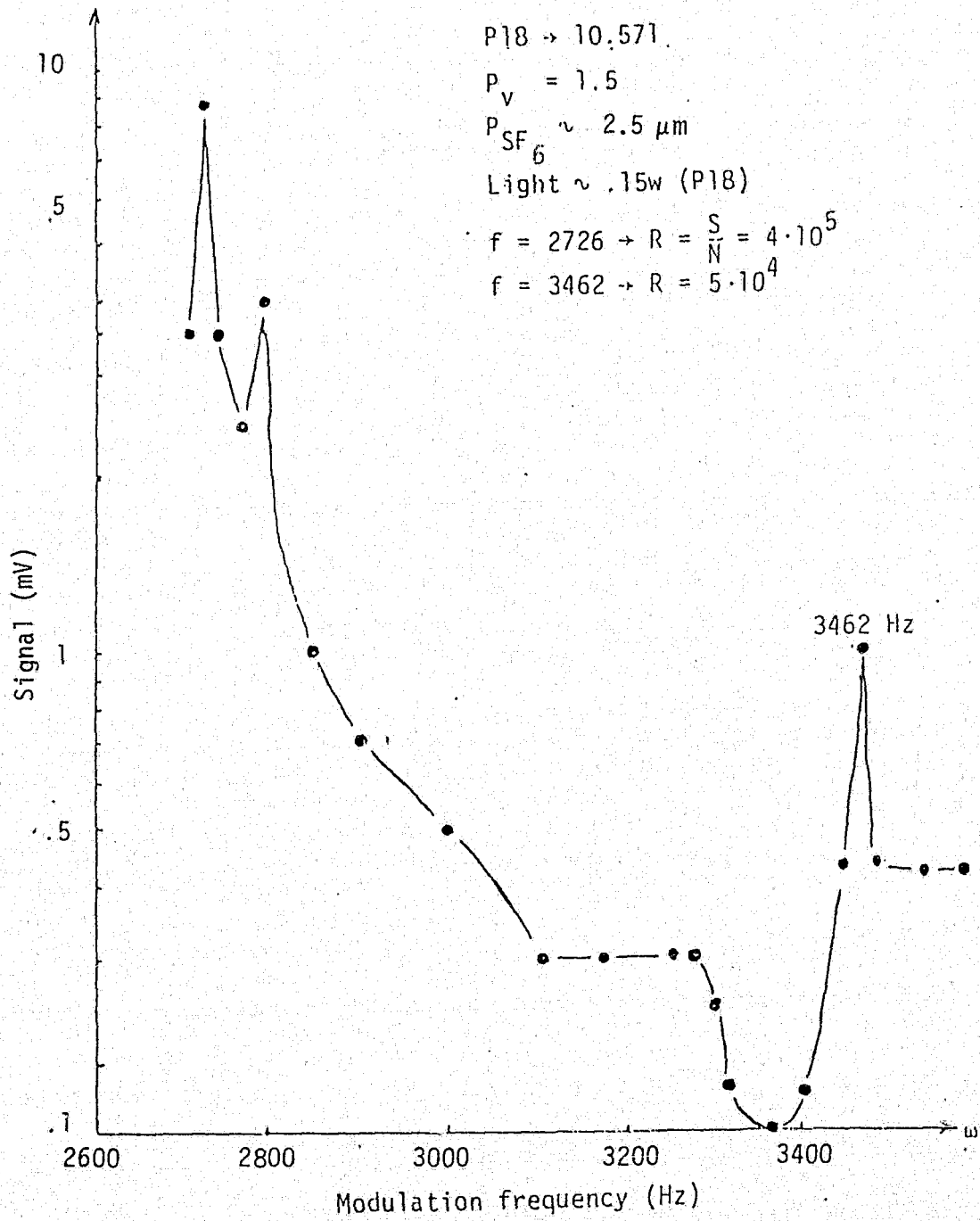


Figure 6. Frequency Response of the Optoacoustic Cell

of the (001)-(100) CO₂ band. The following data were used in the determination:

Laser wavelength = 10.571 micrometers

SF₆ partial pressure [in 1 atmosphere (atm)
of nitrogen (N₂)] = 2.5×10^{-3} Torr

Laser power = 0.15 watt

Chopping frequency = 2726 Herz

Signal-to-noise ratio = 4×10^5

Using $\alpha = 7.3 \times 10^{-4}$ milli Torr⁻¹ cm⁻¹ for SF₆,⁽¹⁾ the sensitivity for a signal-to-noise ratio of unity is 3×10^{-8} cm⁻¹ watt⁻¹.

Since the detected optoacoustic signal is a function of the absorption coefficient of the gas, the laser power, and the cross-section for conversion of absorbed energy to acoustic energy for the particular molecular system being studied, and is not otherwise dependent on the wavelength of the exciting light, no calibration was made for the cell at CO wavelengths. It should be observed that the calibration for SF₆ at 10.571 micrometers is not necessarily valid for all other molecules because the portion of internal vibrational energy which is converted to kinetic energy may vary among different molecular species.

3. Description of Cell

The optoacoustic detector used in this work is an acoustically resonant device. The cell is constructed of brass and aluminum, with appropriate gasketing and valves to permit

evacuation to pressures on the order of 1 Torr. The optical windows at each end of the cell are of NaCl. Since it is known that polar molecules, such as explosives, tend to be adsorbed onto the surface of materials such as those used in this cell, heater coils were provided to enable operation at elevated temperatures. All measurements were made with a small sample placed inside the cell, so no provisions were made to permit continuous air flow.

A dimensional drawing of the cell is shown in Figure 7.

b. Measurement Procedure

Prior to making measurements, the cell was cleaned with methanol to remove surface dirt, and air dried overnight. The cell was then evacuated to a pressure of less than 1 Torr and filled with high purity N_2 to a pressure of 1 atm. A spectrum was then obtained using the same wavelengths and intensities which were to be used for the explosives measurements. This background spectrum, which was nonzero in the 6 micrometer region, was subtracted from each explosives spectrum. A small explosives sample (typically ~1 milligram) was then placed inside the cell and the cell was again evacuated and filled with high purity N_2 to 1 atm and the spectrum was obtained. The sample was removed, the cell was flushed with N_2 , evacuated and refilled with N_2 . The background spectrum was repeated to ensure that no explosive remained in the cell before a new sample

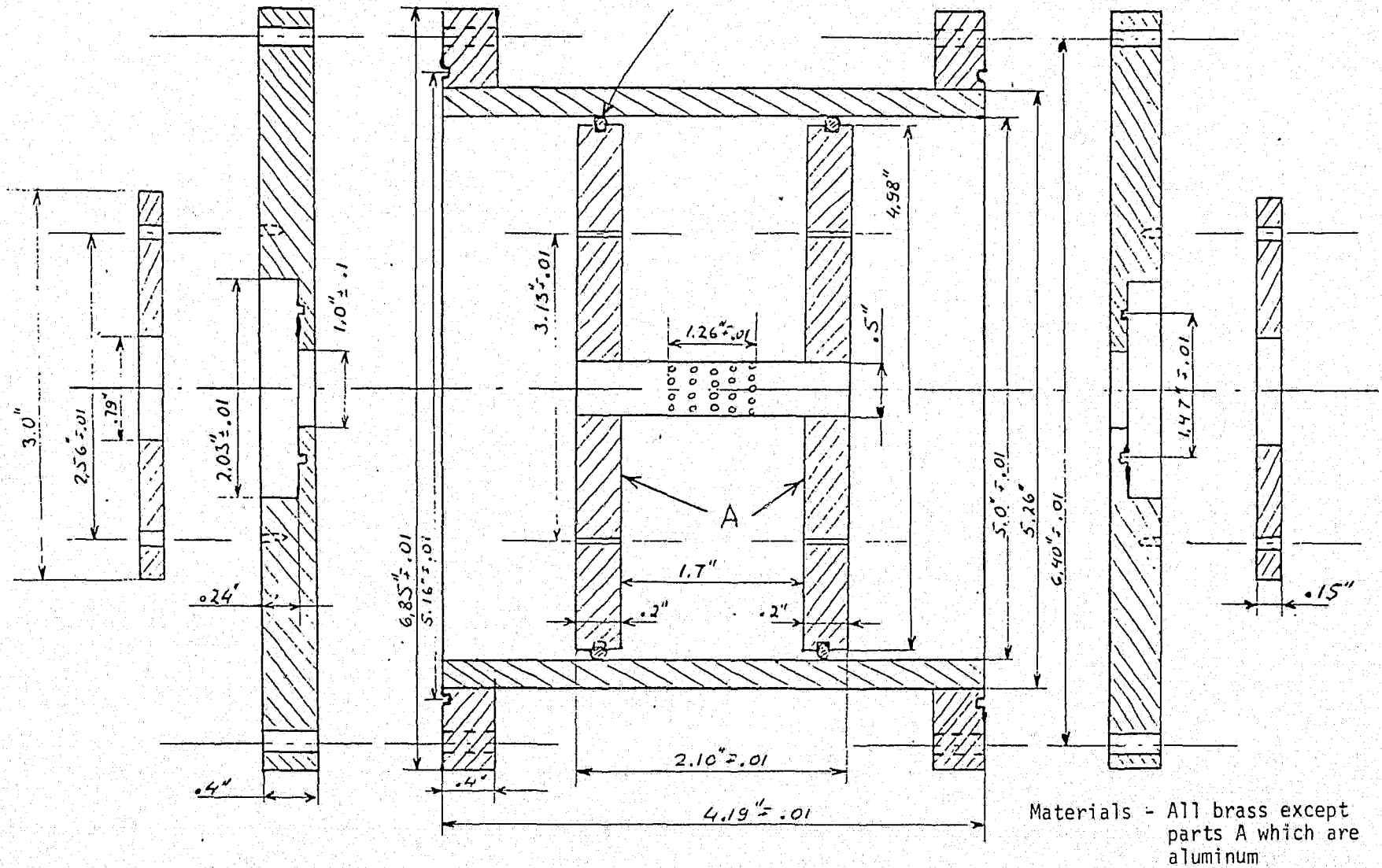


Figure 7. Drawing of the Optoacoustic Cell

was inserted. Measurements were made with the cell at room temperature or at 45 degrees Celsius ($^{\circ}\text{C}$).

c. Sample Handling

1. Methods for Verification of Purity of Explosives and Interference Gases

(a) Explosives

No local verification of purity of explosives was undertaken. The samples were used as obtained from Austin Powder Co., McArthur, Ohio.

(b) Interference Gases

No local verification of purity of the interference gases was undertaken. The gases, diluted in high purity N_2 to the concentrations given below, were supplied by Air Products and Chemicals, Tamaqua, Pa. Analytical reports were supplied with the gases.

Gas	Concentration in N_2 [parts per million (ppm)]
NO	16
NO_2	6.1
CH_4	10
C_4H_{10}	8.8

2. Precautions Taken to Ensure that Contamination
Did Not Occur

To ensure noncontamination of the samples, the explosives were stored in clean metal or glass containers at all times. The gases were stored as supplied in high pressure cylinders.

As a check of noncontamination, no changes in spectra were observed during the several months of the measurement phase of the program.

3. Methods to Verify Whether or Not Adsorption or
Desorption of Material Occurred Inside Cell

(a) Adsorption or Desorption of Explosives

Rakaczky, et al.,⁽²⁾ have reported that explosives vapors are adsorbed by many materials, including those used in the construction of the cell. Qualitative evidence that this was in fact occurring was obtained in Case Western Reserve University's early experiments. To minimize the problems arising from this effect, namely loss of samples, the cell was normally operated at an elevated temperature (45°C). Although heating did not eliminate the adsorption problem, it did significantly reduce its impact. In addition, no effects resulting from desorption of explosives or other materials from the cell walls were observed. If significant desorption were

occurring, the explosives spectrum would have been observable after removal of the bulk sample from the cell.

(b) Adsorption or Desorption of Foreign Materials

Had adsorption and subsequent desorption of foreign materials occurred in the cell, the spectra of such materials would have been included in the background spectra taken with high purity N_2 . Since the background spectra were subtracted from the explosives spectra, no net effect of such materials was contained in the explosives spectra.

4. Methods Used to Detect Possible Contamination

As indicated in Par. c.2, no changes in spectra were observed during the several months of the measurement phase of the program.

d. Saturation Investigation

Linearity of the signal with respect to the incident radiation power level is of interest, since interpretation of data is simplified if it can be shown that increase in population density would merely result in a proportional increase in the magnitude of the optoacoustic signal. Similarly, spectra of interfering species can then be added to the spectra of explosives vapors in a linear manner. To investigate this possibility, optoacoustic signals for NG and air were obtained at 20 different CO_2 transition wavelengths in the 10 to 11 micrometer

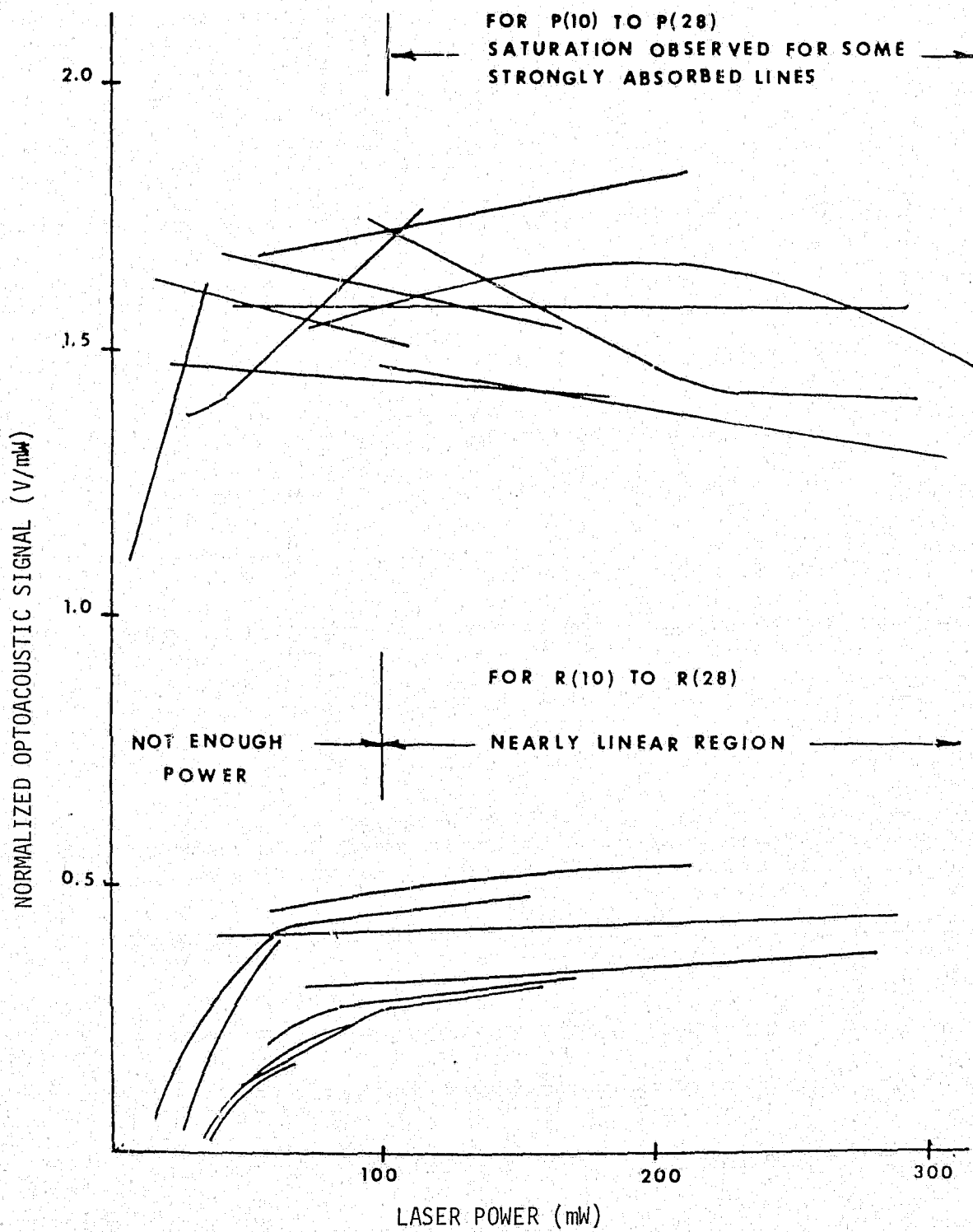


Figure 8. Test for Linearity Using 20 CO₂ Laser Lines

wavelength region for incident power levels ranging from 20 to 350 milliwatts. The normalized signals are plotted versus power level in Figure 8. At low power levels, "dead zone" behavior could be detected; in the 60 to 300 milliwatt range, the normalized response curves were reasonably flat indicating linear response. There seemed to be indication of saturation for some of the highly absorbed lines. The overall behavior indicates, however, that linear superposition of signals would not result in grossly misleading conclusions.

Similar saturation measurements were not made in the 6 micrometer region for two reasons. First, although such measurements were attempted, the CO laser did not produce enough output power for saturation to be observable and, second, the results of the optoacoustic investigation indicated that 6 micrometer radiation is not appropriate for use in an explosives detection device. No theoretical calculations of saturation parameters were made, therefore no comparison with theory was made.

Minimum detectable concentrations of each of the three explosives for which meaningful spectra were obtained have been calculated from the data obtained in this program and the noise-determined minimum detectable signal of 0.15 microvolts. These calculated results are presented in Table 2. In these calculations it was assumed that measurement on the four most strongly absorbed laser lines is sufficient for detection and identification of the vapor. Laser power of 10 milliwatts, at 6 micrometers, and 100 milliwatts

Table 2. Minimum Detectable Explosive Concentration
Using Four Wavelengths

Wavelength (Micrometers)	Explosive	Min. Det. Conc.* (ppm vapor)
6	NG	0.24×10^{-1}
	EGDN	2.5
	DNT	220.
9	NG	0.055×10^{-2}
	EGDN	2.5
	DNT	16.
11	NG	0.28×10^{-2}
	EGDN	1.5

* Interference-free conditions.

at both 9 micrometers and 11 micrometers, has been assumed. These powers were selected to ensure that no saturation occurred.

e. Characterization of CO and CO₂ Lasers

1. CO Laser

(a) The gas mixture contained CO, N₂, xenon (Xe) and helium (He) in the volumetric ratio CO:N₂:Xe:He = 1:1:0.5:13.

(b) The amplitude stability of the output power was approximately $\pm 1\%$ over a 5 minute period.

(c) Once the laser was set to a particular transition, wavelength instability was less than ± 0.0001 micrometer, which was the resolution of the monochromator used in the wavelength determination.

(d) The electrical discharge was in two sections, the voltage and current in each being 8 kilovolts and 6 milliamperes.

(e) The discharge was cooled by a coolant jacket through which methanol at -75°C was circulated.

(f) The cavity consisted of a 10 meter radius of curvature germanium mirror coated for 95% reflectivity at 5.5 micrometers, and a 240 lines/millimeter gold replica diffraction grating on a copper substrate. The reflector spacing was 1.08 meters.

(g) The discharge tube had an active length of 0.75 meter and an inside diameter of 1.2 centimeters. The laser windows were $1.9 \times 3.8 \times 0.5$ centimeter calcium fluoride (CaF_2) crystals.

2. CO₂ Laser (Flowing Gas)

(a) The gas mixture contained CO₂, N₂ and He in the volumetric ratio CO₂:N₂:He = 1:3:16.

(b) The amplitude stability of the output power was approximately $\pm 1\%$ over a 5 minute period.

(c) Once the laser was set to a particular transition, wavelength instability was less than ± 0.0001 micrometer, which was the resolution of the monochromator used in the wavelength determination.

(d) The electrical discharge was in two sections, the current in each being 10 milliamperes. Discharge voltage was not measured.

(e) The discharge tube was cooled by a water jacket through which tap water was circulated.

(f) The cavity consisted of a 4 meter radius of curvature germanium mirror coated for 80% reflectivity at 10.6 micrometers, and a 150 lines/millimeter original diffraction grating ruled on aluminum. The reflector spacing was 1 meter.

(g) The discharge tube had an active length of 0.61 meter and an inside diameter of 1 centimeter. The laser windows were $1.9 \times 3.8 \times 0.5$ centimeter NaCl crystals.

3. CO₂ Laser (Sealed)

(a) The gas mixture contained $^{13}\text{C}^{16}\text{O}_2$, CO, Xe and He in the volumetric ratio $^{13}\text{C}^{16}\text{O}_2:\text{CO}:\text{Xe}:\text{He} = 7:7:1:15$.

(b) The amplitude stability of the output power was approximately $\pm 1\%$ over a 5 minute period.

(c) Once the laser was set to a particular transition, wavelength instability was less than ± 0.0001 micrometer, which was the resolution of the monochromator used in the wavelength determination.

(d) The electrical discharge was in two sections with the current in each being 6 milliamperes.

(e) The discharge tube was cooled by a water jacket through which tap water was flowed.

(f) The cavity consisted of a 2 meter radius of curvature germanium mirror coated for 85% reflectivity at 10.6 micrometers, and a 150 lines/millimeter original diffraction grating ruled on aluminum. The reflector spacing was 1 meter.

(g) The discharge tube had an active length of 0.61 meter and an inside diameter of 1 centimeter. The laser windows were $1.3 \times 0.50 \times 0.08$ inch zinc selenide (ZnSe) crystals.

(h) The discharge tube and cavity construction for this laser were identical to that for the flowing CO_2 laser.

2. Reproducibility and linearity of signals. A measure of the quality of the data obtained in this investigation was obtained by detecting NG in the air using 11 different CO_2 lines in the 10.6 micrometer wavelength region, all at the 50 milliwatt power level. Each of the readings was repeated four times, after all parameters had been adjusted arbitrarily to other readings, and then reset to the original values. The results obtained from that exercise are shown in Table 3. It is seen that the root mean square value of the deviation from perfect reproducibility is 4.8%. The average is closer to 3%, there being two large errors, 9.6% and 5.9%, which are responsible for the root mean square deviation being larger. It is estimated that, with electronically controlled plasma current modulation rather than mechanical modulation, with appropriate narrow band filtering at the pre-amp stage and with feedback control on the laser power supply, this type of error can be reduced to less than 1.5%.

3. Initial considerations of vapor pressure and absorption spectra. Standard, moderate-resolution infrared-absorption spectra were collected for the four explosives, NG, EGDN, DNT and TNT, as well as for some additional commercial preparations such as PETN, TOVEX and ROX.

Table 3. Analysis of Reproducibility of Data - NG and Air, 50 Milliwatts Power

Line	λ	S_1	S_2	S_3	S_4	\bar{S}	$(\overline{(S-\bar{S})^2})^{1/2}$	$\frac{(\overline{(\Delta S)^2})^{1/2}}{\bar{S}} \times 100 = \delta$
P24	11.193	2.2	2.1	2.30	2.30	2.23	.083	3.7%
P22	11.171	2.2	2.3	2.20	2.10	2.20	.070	3.2
P20	11.149	2.4	2.3	2.20	2.20	2.28	.083	3.6
P18	11.127	2.4	2.38	2.30	2.20	2.32	.078	3.3
P16	11.106	2.1	2.20	2.10	2.10	2.13	.043	2.0
P14	11.085	2.3	2.30	2.20	2.20	2.25	.050	2.2
R14	10.816	.64	.60	.60	.60	.61	.021	3.5
R16	10.800	.50	.52	.44	.44	.475	.046	9.6
R18	10.783	.46	.36	.44	.44	.425	.038	5.9
R20	10.768	.46	.46	.44	.44	.45	.010	2.2
R22	10.752	.36	.36	.38	.36	.365	.008	2.3

$$(\delta^2)^{1/2} = 4.8\%$$

Analysis of Reproducibility of Data

NG + Air 50 mW Power

A summary of the absorptions of interest in the present context is provided schematically in Figure 9. Wavelength regions at which discrete laser outputs can be obtained are also indicated in this figure.

Measured and/or extrapolated values for the vapor pressures of the four explosives of principal interest were obtained from the literature.^(3, 4) These values, shown in Figure 10, indicate that at room temperature, equilibrium number densities are 1.25×10^{14} , 5.28×10^{14} , and 1.25×10^{12} per cubic centimeter for EGDN, DNT and NG, respectively.

4. Optoacoustic spectra of explosives. The original contract specified that spectra of the explosives alone were also to be investigated. Initially this was done for three explosives, but no signals were obtained. Previous experience with other gases had indicated that, whereas high resolution spectra could be obtained with gases at pressures less than 1 Torr, the optoacoustic signal was usually three or four orders of magnitude smaller than when a carrier gas was used with the sample. In addition, in the context of the intended application, the optoacoustic signal of interest would be that generated with the explosives vapor in air. In view of these considerations, it was agreed by both Case Western and Aerospace that all optoacoustic spectra would be obtained with dry N_2 .

In practice, the commercially supplied dry N_2 yielded a background optoacoustic signal in the 6 micrometer wavelength region, not characteristic of water vapor but similar to that of NO_2 . This background was subtracted from the explosives vapor optoacoustic spectra in all cases.

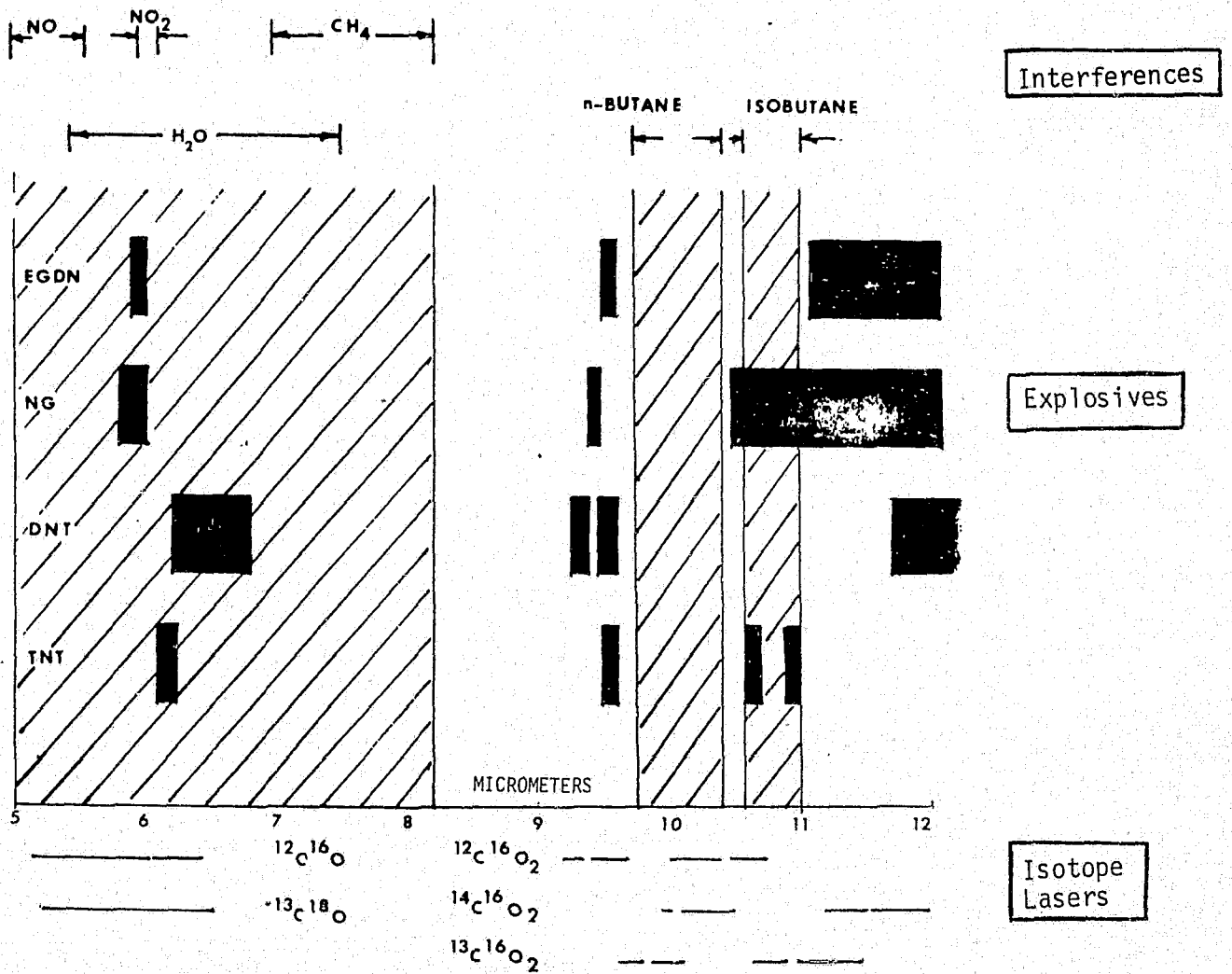


Figure 9. Schematic Representation of Spectral Distribution of Absorptions of Explosives and Interfering Species (Compared with Bands Available from Various Isotope Lasers)

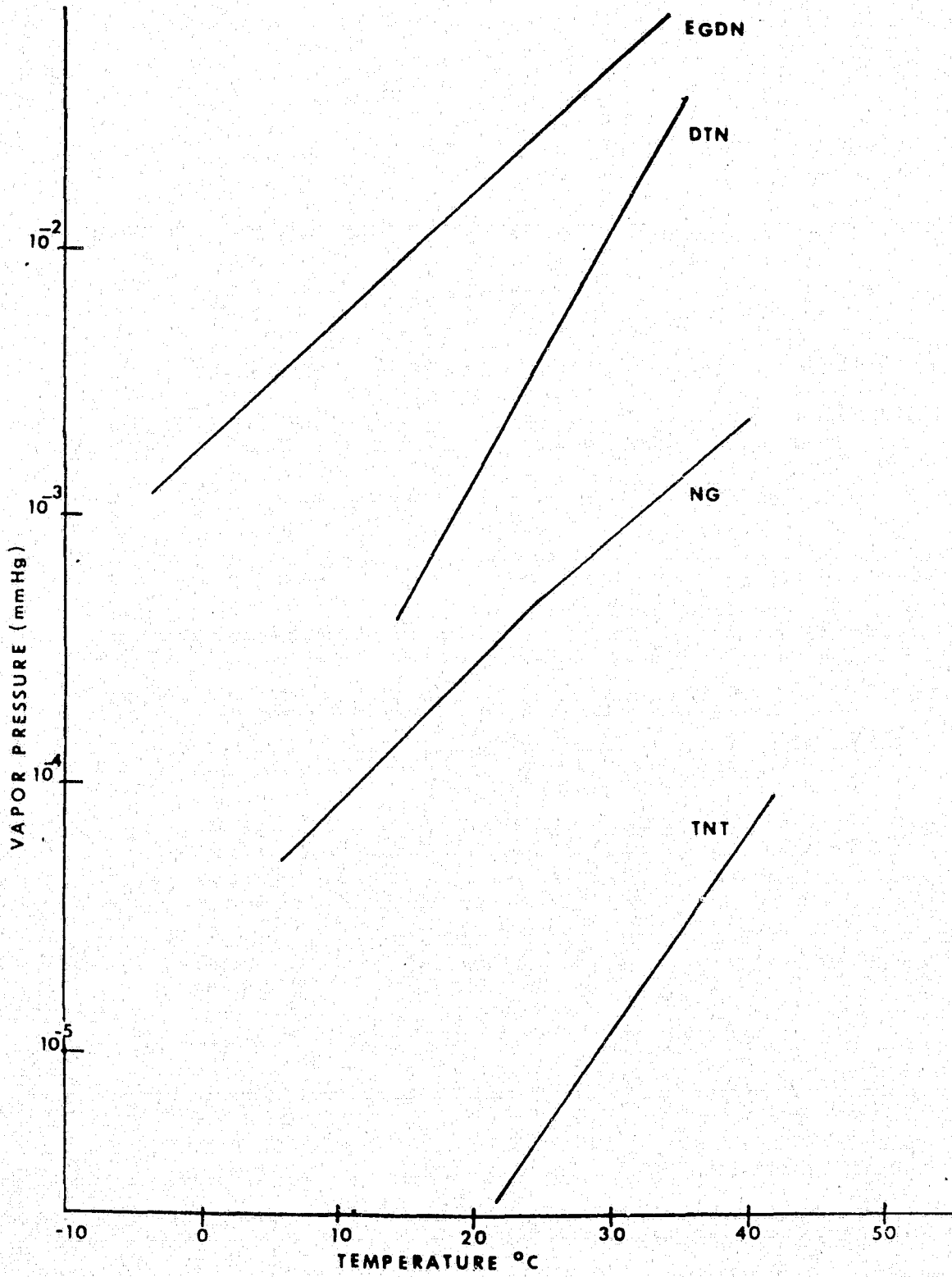


Figure 10. Vapor Pressure of Explosives

The normalized spectra for explosives and interferences measured in the 6, 9 and 11 micrometer regions are collected and presented in Appendix B.

Optoacoustic spectra for the 6 micrometer wavelength region for the vapors of NG, EGDN and DNT are shown in Figures B-1, B-2, and B-3. The average laser power, measured at the input of the cell was 10 milliwatts at each wavelength. Spectra of TNT, RDX, PETN and TOVEX are shown in Figures B-4, B-5, B-6, and B-7, respectively. The reader is cautioned at this point that comparison of these spectra with that of water vapor suggests that in all four cases, the observed spectra are primarily due to water vapor. For RDX, PETN and TOVEX, the water vapor signal is too large to be due to contamination by water in the laboratory air. It is concluded that water is a significant contaminant in these explosives and is the major emitted vapor. The spectrum for a low NG content dynamite is shown in Figure B-8. Data shown in these figures are also given in numerical form in Table 4.

Optoacoustic spectra for the 9 micrometer wavelength region for vapors of NG, EGDN, DNT, dynamite and black powder are shown in Figures B-9, B-10, B-11, B-12, and B-13, respectively. The corresponding data for NG, EGDN and DNT are given in Table 5.

In the 11 micrometer wavelength region, optoacoustic spectra were obtained for vapors of NG and EGDN for 23°C and for 45°C. The spectra are shown plotted in Figures B-14, B-15, B-16, and B-17, respectively, and the corresponding data are given in numerical form in Table 6.

Table 4. Explosive Optoacoustic Spectra (Microvolt per Milliwatt) in the 6 Micrometer Region

<u>WAVELENGTH</u> <u>(Micrometers)</u>	<u>NG</u>	<u>EGDN</u> <u>+10%NG</u>	<u>DNT</u>	<u>TNT</u>	<u>TOVEX</u>	<u>RDX</u>	<u>PETN</u>	<u>DYNAMIC</u>
6.626	0.8	0.8	1.6	0.2	4.8	3.2	2.4	4.8
6.538	0	0	3.0	3.2	12.2	5.2	6.2	6.0
6.465	0	0	1.6	2.1	5.4	3.1	2.8	3.6
6.408	0	0	1.1	0.8	2.8	1.3	1.1	1.5
6.367	0	0	0.8	0.8	2.3	1.3	1.5	2.2
6.312	0	0	0	0	0.3	0.3	0	0
6.258	0	0	0	0	0.5	0.3	0	0
6.213	0	0	0.4	0.5	1.1	1.0	0.2	0.5
6.174	1.0	2.2	2.0	5.8	13.3	5.8	6.0	3.5
6.132	0	1.4	0.3	0.6	2.6	1.1	1.3	2.0
6.063	0.3	3.9	1.3	2.8	6.2	3.6	1.1	3.6
6.002	5.3	60.5	4.6	2.6	10.9	5.3	4.3	7.6
5.941	2.1	41.2	3.2	3.0	8.5	3.5	2.7	6.0
5.880	2.0	3.3	2.9	7.2	16.7	7.2	7.4	7.2
5.837	0.1	1.2	1.1	1.6	6.1	3.1	2.3	3.0

Table 5. Explosive Optoacoustic Spectra (Microvolt per Milliwatt) in the 9 Micrometer Region

<u>Wavelength (Micrometers)</u>	<u>NG</u>	<u>EGDN</u>	<u>DNT</u>
9.711	1.7	2.5	0.8
9.655	1.7	2.2	0.6
9.601	2.2	3.2	0.8
9.550	2.2	5.0	1.0
9.501	2.2	5.0	1.1
9.455	-	4.0	1.0
9.352	0.75	2.0	.55
9.303	0.5	1.5	.35
9.247	0.25	1.0	.30
9.217	-	0.5	.20

Table 6. Explosive Optoacoustic Spectra (Microvolt per Milliwatt)
in the 11 Micrometer Region

<u>Wavelength (Micrometers)</u>	<u>NG(45°C)</u>	<u>NG(23°C)</u>	<u>EGDN(45°C)</u>	<u>EGDN(23°C)</u>
11.194	6.5	0.4	6.2	0.6
11.149	5.2	0.4	7.0	0.6
11.107	4.6	0.4	6.5	0.55
11.065	3.3	0.35	5.3	0.5
10.850	-	0.12	-	0.23
10.833	1.5	-	1.5	-
10.800	1.3	0.12	0.8	0.23
10.753	1.0	0.12	0.5	0.23

B. Investigation of Interfering Species

It was agreed that the interfering species to be investigated would be butane, methane, NO_2 , NO and water vapor. These were investigated in both the 6 micrometer and 9 micrometer wavelength regions.

For the 6 micrometer wavelength region, the concentrations for the samples used are listed in Table 7 and optoacoustic spectra data are listed in Table 8. The spectra are shown plotted in Figures B-18 through B-22.

In the 9 micrometer wavelength region, none of the listed interfering species yielded any optoacoustic signal except for butane. The optoacoustic spectrum for butane is shown in Figure B-23.

C. Determination of Optoacoustic Spectra of Explosives Vapor in the Presence of Interfering Species

The extensive exploration of additional transitions in the 9 micrometer and 11 micrometer wavelength region did not leave sufficient time to perform all the tasks of the contract to the letter. However, all the required spectra of the listed interfering species had been obtained, and the results of the investigation of the validity of superposition of spectra allow conclusions to be drawn from the two separate families of spectra. Furthermore, and this was really the most compelling reason, data listed in Tables 7 and 8 clearly show that interference due to water vapor renders the 6 micrometer wavelength region marginal at best for optoacoustic detection of explosives vapors. Although interference from NO_2 alone might threaten to render detection of DNT ineffective, the added effect of the omnipresent water vapor is much, much worse. Therefore, for the

Table 7. Concentration of Interfering Species
(partial pressure) in Nitrogen

<u>Interfering Species</u>	<u>Concentration</u>
NO	16 ppm
NO ₂	6.1
CH ₄	10
C ₄ H ₁₀	8.8
Water Vapor	~ 57,000

Table 8. Pollutant Optoacoustic Spectra (Microvolt per Milliwatt) in the 6 Micrometer Region

<u>Wavelength (Micrometers)</u>	<u>Butane</u>	<u>Methane</u>	<u>Nitric Oxide</u>	<u>Nitrogen Dioxide</u>	<u>Water</u>
6.626	2.50	0.17	2.38	9.17	12.5
6.538	1.67	0.67	2.37	0	28.0
6.465	2.50	1.59	0.39	5.50	15.0
6.408	2.40	0.75	1.08	3.08	8.5
6.367	0.72	0.90	0.28	2.00	7.5
6.312	0.13	0.47	0.25	1.16	1.0
6.258	0.20	0.09	0.67	0.94	1.5
6.213	0.25	0.29	0.66	2.01	3.5
6.174	1.75	1.08	1.87	8.37	33.5
6.132	0.30	0.21	0.25	1.75	9.0
6.063	0.28	0.42	0.34	3.43	20.0
6.002	1.43	0	0	4.17	30.0
5.941	0.91	0.19	0.22	3.18	22.0
5.880	1.16	0.91	0.14	8.64	50.0
6.837	0.75	2.10	0	9.44	20.0

6 micrometer wavelength region, the optoacoustic spectra of vapors of EGDN, NG and DNT in the presence of water vapor have been synthesized from actual (but separately determined) optoacoustic spectra. Figure B-24 illustrates that it is relatively easy to detect EGDN at room temperature at 50% relative humidity. As shown in Figures B-25 and B-26, the situation is less favorable for NG, and circumstances are definitely not favorable for DNT. A relative humidity of 50% would be unacceptable for the last case.

CHAPTER IV. FEASIBILITY DETERMINATIONS

In this chapter, results are reported of an evaluation of whether it is indeed feasible to use optoacoustics to detect the presence of explosives. The evaluation is based on data reported in previous sections, on additional data to be reported in this section and on experience obtained during field operation of a portable optoacoustic unit.

Some of the basic considerations included in the evaluation are those of:

- a. Intrinsic optoacoustic efficiency
- b. Basic difficulties due to interference
- c. Ultimate limitations imposed by technology
- d. Cost, reliability and ease of operation.

Table 9 lists quantities which serve as figures of merit insofar as optoacoustic detection is concerned. They are the maximum normalized optoacoustic signals detected (that is, microvolts of signal per milliwatt of incident radiation) for a vapor with a concentration of 1 ppm. The actual figures listed in Table 9 are valid only for the specific CO transitions used in this investigation.

A. Optoacoustic Efficiency

Referring to Table 9, it is seen that the optoacoustic efficiencies of the explosives EGDN and NG are comparable to those of smaller molecules, but that of DNT is lower. It is not possible to conclude on the basis of these data alone whether ring structures do enhance internal vibrational

Table 9. Optoacoustic Efficiency of Explosives and Interfering Species at 6 Micrometers

Molecule	Max. Normalized Optoacoustic Signal ($\mu\text{V}/\text{mW}$)	Molecular Concentration (ppm)	Max normalized Optoacoustic Signal per ppm ($\mu\text{V}/\text{mW}/\text{ppm}$)
NG	5.3	0.62	8.55
EGDN	60.5	53	1.14
DNT	4.6	92	0.05
NO	2.38	16	0.15
NO ₂	9.44	6.1	1.55
H ₂ O	50	47 x 10 ³ (39°C, 50% RH)	0.001
CH ₄	2.1	10	0.21
Butane	2.5	8.8	0.28

Results calculated using the following data:

Explosive	Number density at 45°C for vapor in equilibrium with explosive
NG	1.43 x 10 ¹³ cm ⁻³
EGDN	1.22 x 10 ¹⁵
DNT	2.13 x 10 ¹⁵

1 ppm in air at 1 atm, 45°C corresponds to 2.3 x 10¹³ cm⁻³

RH = relative humidity

energy trapping, resulting in lower optoacoustic efficiency, or whether the lower value for DNT is due to smaller absorption coefficients. However, the values listed in Table 9 indicate that there is nothing drastically wrong with the optoacoustic response of the explosives EGDN, NG and DNT. Since most of the 6 micrometer wavelength region work was carried out with only about 10 milliwatts of incident power, there is much opportunity for enhancement of the signal. Similar conclusions are equally valid for the data obtained in the 9 micrometer and 11 micrometer wavelength regions.

B. Interference

As mentioned in previous sections, interference may arise because of other molecular systems present in the environment or because of substances entrained with the explosives. In the 6 micrometer wavelength region, NO, NO₂ and water vapor give rise to interference of varying degrees of difficulty depending on the explosives involved. However, it is water vapor which is most troublesome. It is interesting to note that, for the 6 micrometer transitions used in this investigation, water is in fact very optoacoustically inefficient, the signal being 0.001 $\mu\text{V}/\text{mW}/\text{ppm}$ as compared with 8.55 $\mu\text{V}/\text{mW}/\text{ppm}$ for NG, 1.114 $\mu\text{V}/\text{mW}/\text{ppm}$ for EGDN and 0.05 $\mu\text{V}/\text{mW}/\text{ppm}$ for DNT, respectively. However, there are many water molecules in air, even at "low" relative humidity, and the resulting interference is not negligible. (See Figure B-26, for example.)

We note, however, that if the water vapor is present in the environment, the optoacoustic signal from that background can be determined

separately and subtracted from the combined signal. In practice this could be carried out using two optoacoustic cells. A single incident beam would be split and the two portions directed into two detector cells. The resulting water vapor background signals would be adjusted so that no coherent alternating current optoacoustic signal is obtained in the absence of the explosive. The explosives optoacoustic signal alone is obtained as the laser tuned across (say) six different transitions. This same technique can be used to alleviate the interference effects due to other environmental interfering species. By use of this common mode rejection scheme, it is anticipated that all three explosives, NG, EGDN and DNT, can be detected for conditions equivalent to the vapor being in equilibrium with the explosive (for NG, approximately 1 ppm; for EGDN, about 75 ppm; and for DNT, about 50 ppm).

Of much greater concern are instances where the water seems to be entrained in the explosive, and the vapor pressure of the explosive itself is low so that the water vapor optoacoustic signal dominates the output. This seems to be the situation for the explosives RDX, PETN and TOVEX. In the laboratory, there was some thought of removing the water from the explosives so that the optoacoustic signals of the explosives alone could be obtained. However, inasmuch as some of these explosives are normally prepared in the form of water slurries and, since, in the contemplated use at airports, etc., there would not be the opportunity to desiccate all luggage presented for inspection, this elaborate approach was abandoned for more practical ways of circumventing the interference problem. This was the

principal reason for the additional work carried out at 9 micrometers and 11 micrometers. Investigations at these higher wavelengths showed no interference due to NO, NO₂, CH₄ or water vapor. However, higher molecular weight hydrocarbons may be troublesome, and butane constitutes an example. Again, dual cell, common mode rejection techniques may be used to reduce the effects of environmental interfering species in the 9 to 12 micrometer wavelength region.

C. System Design Considerations

The principal components of an optoacoustic detector system are a laser, a radiation chopper, the detector cell itself and associated power supplies and signal processing electronics. Of all these ingredients, the only questionable item is the availability of a long-lived, sealed-off, extended tuning range CO laser. More specifically, the operating life expectancy should be above 5000 hours in the sealed-off, dry ice cooled mode; power should be at least 1 watt when operated with a diffraction grating or its equivalent; and gain should be sufficiently high so that the tuning range extends to at least 6.6 micrometers. Although such a laser might be available at one or more laboratories, there is no accumulated experience regarding long-lived, sealed-off CO lasers. In contrast to this, there is now sufficient collective experience to indicate that long-lived, sealed-off CO₂ lasers with mixed isotopes and extended tuning range can readily be implemented. This is a good reason for giving serious thought to the 9 to 12 micrometer wavelength region.

The detector cell is inherently a simple device, and there is information in the open literature regarding the principles guiding the design

of such cells. Each laboratory will, of course, develop its own preferred practice in cell design, resulting in real or imagined improved performance. The results of this study suggest that the inner surfaces of the cell be heated to reduce adsorption, but the temperature should not be so high as to degrade microphone performance. It is important to check the electronic saturation characteristics of such microphones.

Most of the data in the course of this investigation were taken using a mechanical light chopper. Mechanical choppers are adequate for the purpose, but are often not very stable in the chopping frequency, do not provide simple harmonic modulation and often cannot provide modulation at sufficiently high frequencies. At Case Western, it is found that more satisfactory modulation can be obtained via direct modulation of the laser plasma discharge current. Higher modulation frequencies and smaller cells can be obtained in this manner. Feedback control can also be used to ensure sinusoidal modulation. Reverting to the topic of cell design, it is worth mentioning at this point that some cells have high acoustic quality factors (Q), but are not very sensitive to minor frequency deviations away from the resonant frequency. Other cells of more classic design have the disadvantage of having such sharp resonance curves that elaborate frequency stabilization is required if noise is to be kept to acceptable levels.

Laser-excited optoacoustic detector systems contemplated in this study are inherently simple systems. A rough estimate indicates that such systems may be produced for sale at a unit price of less than \$25,000.

This price would vary somewhat depending on what additional signal processing and/or display features are required. Again CO systems might be troublesome because of the possible need for occasional refill. There is no such difficulty with sealed-off, long-lived CO₂ lasers and it would seem that the CO₂ units could be operated by non-technical personnel.

More specifically, a typical CO₂ laser optoacoustic detector system would comprise the following components with the indicated estimated power requirements, sizes and weights:

- a. The laser and cell assembly, including the coolant reservoir, thermoelectric cooler, beam splitter, common mode rejection dual cell assembly, diffraction grating for wavelength tuning and piezoelectric transmission mirror for power optimization. The power requirement is approximately 200 watts, weight is estimated to be less than 50 pounds and dimensions are of the order of 22 × 8 × 8 inches.
- b. The power supply unit includes the high voltage power supply, discharge current modulation control, diffraction grating stepping motor supply and control and cavity dimension optimization supply and control. Dimensions are estimated to be of the order of 18 × 8 × 8 inches. Weight is less than 50 pounds.
- c. The data processing and display unit includes a current (pre) amplifier and a phase-sensitive amplifier with a limited frequency tuning option. Logic for controlling the

tuning sequence of the laser and means for processing the "signature" of the received signal are provided. A simple yes/no type of display (perhaps audio as well as visual) would probably be the principal output device. In addition, a simple "profile" or signature" readout device might also be desirable.

As this phase of the investigation neared the end (as dictated by allotted time and funds), it became clear that the investigation had succeeded in revealing the nature of the possible problems and had also succeeded in establishing the directions in which some limited, additional investigations were indicated. To do the most good in the remaining time, it was agreed by both Case Western and Aerospace that the investigation would not be strictly limited to the exact letter of the contract, but would proceed as rapidly as possible to reveal the possibilities available in the 9 to 11 micrometer wavelength region. For a while, this implied that there would not be an opportunity to carry out the test in public places, such as an airport or a bus station. Fortunately, a semiportable, self-contained CO₂ laser-excited optoacoustic unit (constructed by Case Western Reserve University under separate contract for a local instrument company) was secured and this unit was operated for four days at a local instrument exhibit at the Convention Center in downtown Cleveland. The environment in the hall was excellent for test purposes. Although bringing explosives into the hall was not allowed, the ability to detect SF₆ at 10.6 micrometers amidst all the gasoline fumes and other types of pollution was demonstrated.

This field demonstration was of special significance in view of some additional work carried out at the suggestion of Aerospace. Three types of samples were tested to ascertain if SF₆ emitted by these samples could be optoacoustically detected. As indicated by the results exhibited in Figure B-27, SF₆ was detected in all three cases. The first sample consisted of a metal simulated blasting cap. The SF₆ optoacoustical signal obtained in that case was overwhelmingly large, being 714 μV/mW. The other two samples consisted of Teflon capsules impregnated with SF₆ at an earlier time and estimated to be emitting SF₆ at extremely low rates, perhaps at the rate of 1 to 5 nanoliters per minute. As shown in Figure B-27, positive identification was obtained in both cases, but the profile showed signs of saturation and the intensity of the incident radiation was probably too high for the purpose.

CHAPTER V. RECOMMENDATIONS

It is recommended that this initial promising investigation be followed up so that the following activities and results might be pursued and attained:

- a. Optoacoustic spectra of explosives and of SF₆ be examined carefully in the 9 to 12 micrometer wavelength region with the use of mixed isotope CO₂ lasers. The interference due to hydrocarbons (butane and higher molecular weight), such as those found in jet fuels, needs to be examined.
- b. The dual cell, common-mode rejection technique be developed and used in all future investigations so as to yield more meaningful estimates of irreducible effects of interfering species.
- c. The 6 micrometer wavelength region be re-examined with increased CO power and with the dual cell, common-mode rejection technique.
- d. Detection be carried out with gas flowing through the detector cell.
- e. A field operable system be designed incorporating scanning and power optimization, narrow band filtering and phase sensitive amplification and appropriate signal processing and display.
- f. A prototype of this field operable unit be implemented.

APPENDIX A

A RATE EQUATION DESCRIPTION OF A
TWO-LEVEL OPTOACOUSTIC SYSTEM

In the interest of completeness, we provide here a rate equation description of a simple two-level model of an optoacoustic system. In this model, the molecular system interacts resonantly with incident radiation and transitions between the two levels are stimulated. In addition, de-excitation from the upper level occurs because of fluorescence (spontaneous emission, with rate τ_R^{-1}) and also because of collisions (with rate τ_c^{-1}). The optoacoustic signal is proportional to $N_2 \tau_c^{-1}$, where N_2 is the number of molecules in the upper state per unit volume. The power levels required for excitation, the behavior of the system when near saturation and the desirability of using the second harmonic signal are topics also mentioned briefly in passing.

Let us consider a two-level system, and

Let N = number of molecules/cm³ = $N_1 + N_2$

where N_1 = number of molecules/cm³ in the lower state

and N_2 = number of molecules/cm³ in the upper state

The rate equation description of the system may be written as

$$\frac{dN_1}{dt} = - B_{12} \frac{I \nu}{c} N_1 + B_{21} \frac{I \nu}{c} N_2 + \left(\frac{1}{\tau_R} + \frac{1}{\tau_c} \right) N_2 \quad (A-1)$$

$$\frac{dN_2}{dt} = - B_{21} \frac{I \nu}{c} N_2 + B_{12} \frac{I \nu}{c} N_1 - \left(\frac{1}{\tau_R} + \frac{1}{\tau_c} \right) N_2 \quad (A-2)$$

where $B_{12} = B_{21}$ = Einstein Coefficient For Stimulated
Absorption and Emission

ν = frequency of radiation interacting resonantly
with the molecular system

I_ν = number of photons/cm²/sec of energy $h\nu$

τ_R = radiation lifetime of upper state

τ_c = collisional lifetime of upper state

For convenience these equations can be combined and slightly
rewritten as

$$\frac{d}{dt}(N_2 - N_1) = -B(N_2 - N_1)I_\nu - 2\tau^{-1}N_2 \quad (\text{A-3})$$

where $B = B_{12} \frac{h\nu}{c}$

$$\tau^{-1} = \left(\frac{1}{\tau_R} + \frac{1}{\tau_c} \right)$$

We note in passing that

$$B_{12} = \frac{\pi^2 c^3}{\Delta\nu h\nu^3} A_{21} = \frac{\pi^2 c^3}{\Delta\nu h\nu^3 \tau_R}$$

We may safely assume that steady-state conditions are always
attained, i. e., for any I_ν , the system has ample time to adjust itself
to steady-state conditions appropriate to that value. This means that
we can take

$\frac{d}{dt}(N_2 - N_1) = 0$ and Eq. (A-3) yields

$$N_2 = \frac{BNI_v}{2BI_v + 2\tau^{-1}} \quad (\text{A-4})$$

The acoustic signal is proportional to $N_2\tau_c^{-1}$ and we have, accordingly, that the acoustic signal

$$\propto N_2\tau_c^{-1} = \frac{BNI_v\tau_c^{-1}}{2BI_v + 2\tau^{-1}} \quad (\text{A-5})$$

In the case where the incident radiation is modulated at frequency ω so that

$$I_v = I_o(1 + \delta \sin \omega t) \quad \text{where } 0 \leq \delta \leq 1 \quad (\text{A-6})$$

we can consistently write

$$N_{2c}^{-1} = \frac{BNI_o(1 + \delta \sin \omega t)\tau_c^{-1}}{2BI_o(1 + \delta \sin \omega t) + 2\tau^{-1}} \quad (\text{A-7})$$

Expanding in powers of $\delta \sin \omega t$ and retaining only terms up to the second power of $(\delta \sin \omega t)$, we have

$$\begin{aligned}
N_2 \tau_c^{-1} = & \frac{B N I_o \tau_c^{-1}}{2 B I_o + 2 \tau_c^{-1}} - \frac{4 B^2 I_o^2 N \tau_c^{-1} \delta^2}{[2 B I_o + 2 \tau_c^{-1}]^3} \\
& + \frac{2 \tau_c^{-2} B N I_o}{(2 B I_o + 2 \tau_c^{-1})^2} \delta \sin \omega t + \frac{4 B^2 I_o^2 N \tau_c^{-1}}{(2 B I_o + 2 \tau_c^{-1})^3} \delta^2 \sin 2 \omega t + \dots
\end{aligned}
\tag{A-8}$$

Insofar as the $\sin \omega t$ term is concerned, we see that for very small I_o , $B I_o \ll \tau_c^{-1}$ and

$$\frac{2 \tau_c^{-2} B N I_o}{(2 B I_o + 2 \tau_c^{-1})^2} \delta \rightarrow \frac{1}{2} \left(\frac{\tau_c}{\tau_c} \right)^2 B N I_o \delta
\tag{A-9}$$

But when I_o becomes very large, then

$$\frac{2 \tau_c^{-2} B N I_o}{(2 B I_o + 2 \tau_c^{-1})^2} \delta \rightarrow \frac{1}{2} \tau_c^{-2} \frac{N}{B I_o} \delta
\tag{A-10}$$

It is quite apparent that $B I_o$ should be large but not larger than τ_c^{-1} .

This can be demonstrated also by solving Eq. (A-10) for the optimum value of $B I_o$. Actually $B I_o \equiv \frac{1}{\tau}$ or the reciprocal of the lifetime as specified by interaction with radiation and the optimum condition merely says (qualitatively) that we should not pump harder than we can deplete the upper state by collisional process.

Depending on the partial pressure of the absorbing gas, the presence or absence of other gases, and the influence of wall collisions,

τ might be of the order of, say, 10^{-6} second and it found that saturation sets in at quite low powers of the order of fractions of a watt/cm². This is in agreement with our experience in our high resolution saturation spectra of SF₆ and of I₂¹²⁹.

Furthermore the manner in which saturation occurs is of interest. In Eq. (A-8), the dominant direct current term has I₀ to the same power in the numerator and in the denominator. Unnecessarily high values of I₀ might not bring correspondingly higher signal values but there are no penalties either. This is different for the other terms. In particular, the alternating current term at frequency ω saturates according to I₀⁻¹, and so does the second harmonic term. It is important therefore in practice to avoid using unnecessarily high incident powers.

Scattering and absorption at the window would result in a spurious signal also at a frequency of ω , and it has been suggested that detection of the second harmonic might provide the means for discriminating against that spurious signal. However, from Eq. (A-8) we note that as saturation sets in the two terms have the following behavior

$$\frac{2\tau_c^{-2} B N I_0}{(2B I_0 + 2\tau_c^{-1})^2} \delta \sin \omega t \rightarrow \frac{1}{2} \frac{\tau_c^{-2} \delta}{B I_0} \sin \omega t \quad (\text{A-11})$$

$$\frac{4B^2 I_0^2 N \tau_c^{-1}}{(2B I_0 + 2\tau_c^{-1})^3} \delta^2 \sin 2\omega t \rightarrow \frac{1}{2} \frac{\tau_c^{-1} \delta^2}{B I_0} \sin 2\omega t \quad (\text{A-12})$$

The amplitude of the second harmonic term is smaller by a factor of τ_c^{-1} which can be as large as 10^7 !

APPENDIX B

COLLECTION OF OPTOACOUSTIC SPECTRA OF EXPLOSIVES
AND INTERFERENCES TAKEN AT 6 μm (CO LASER)
AND 9 AND 11 μm (CO₂ LASER)

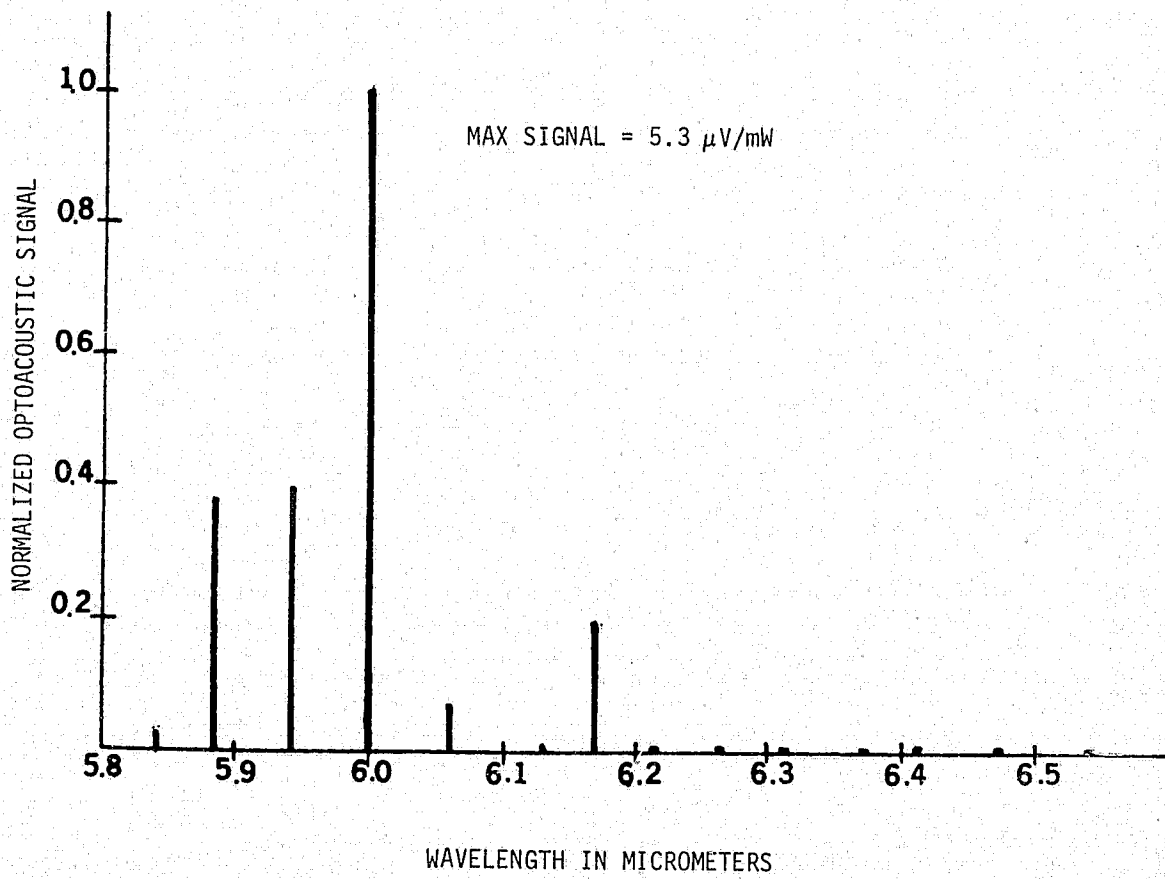


Figure B-1. Optoacoustic Spectrum of NG at 6 Micrometers (45°C)

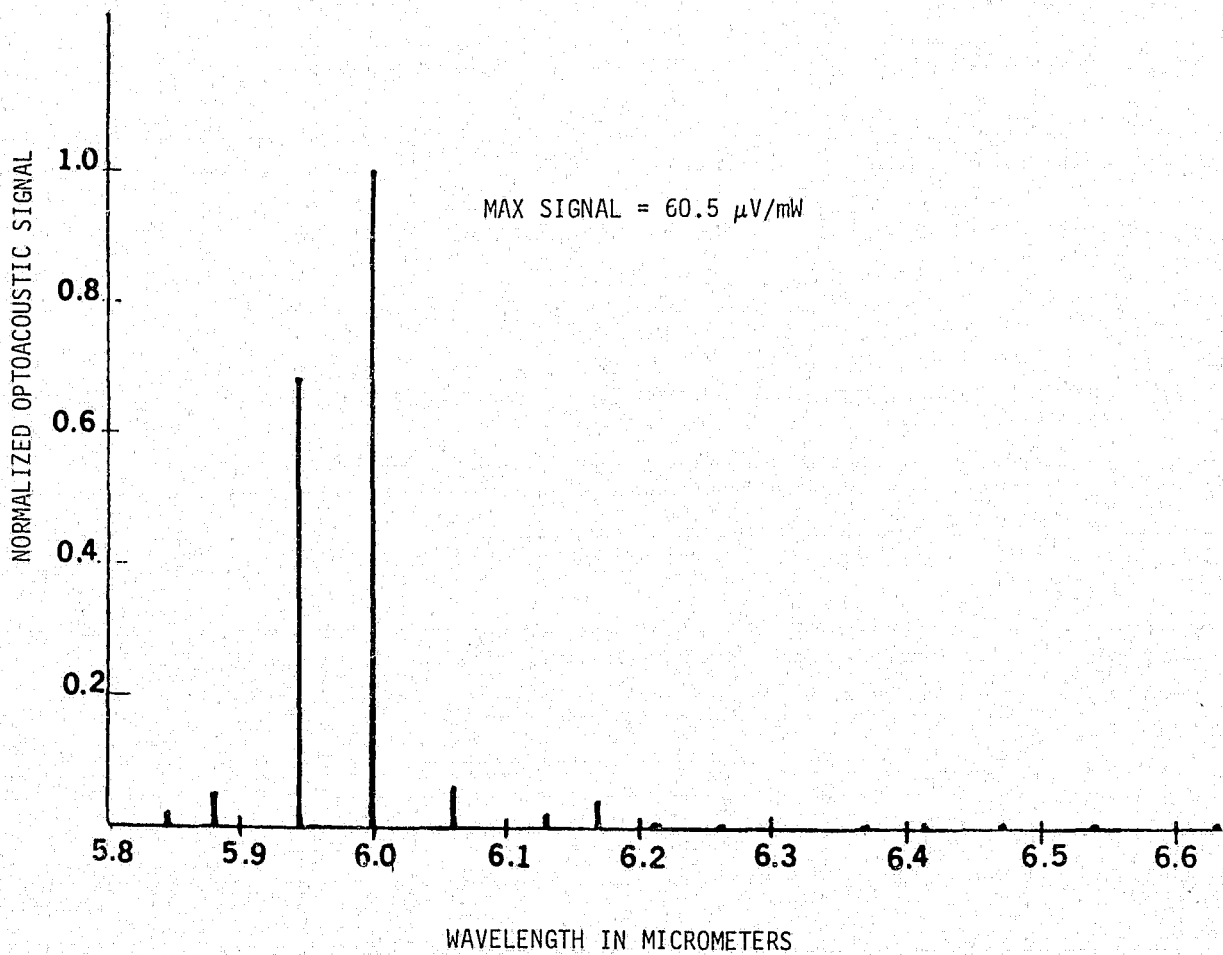


Figure B-2. Optoacoustic Spectrum of EGDN (10% NG) at 6 Micrometers (45°C)

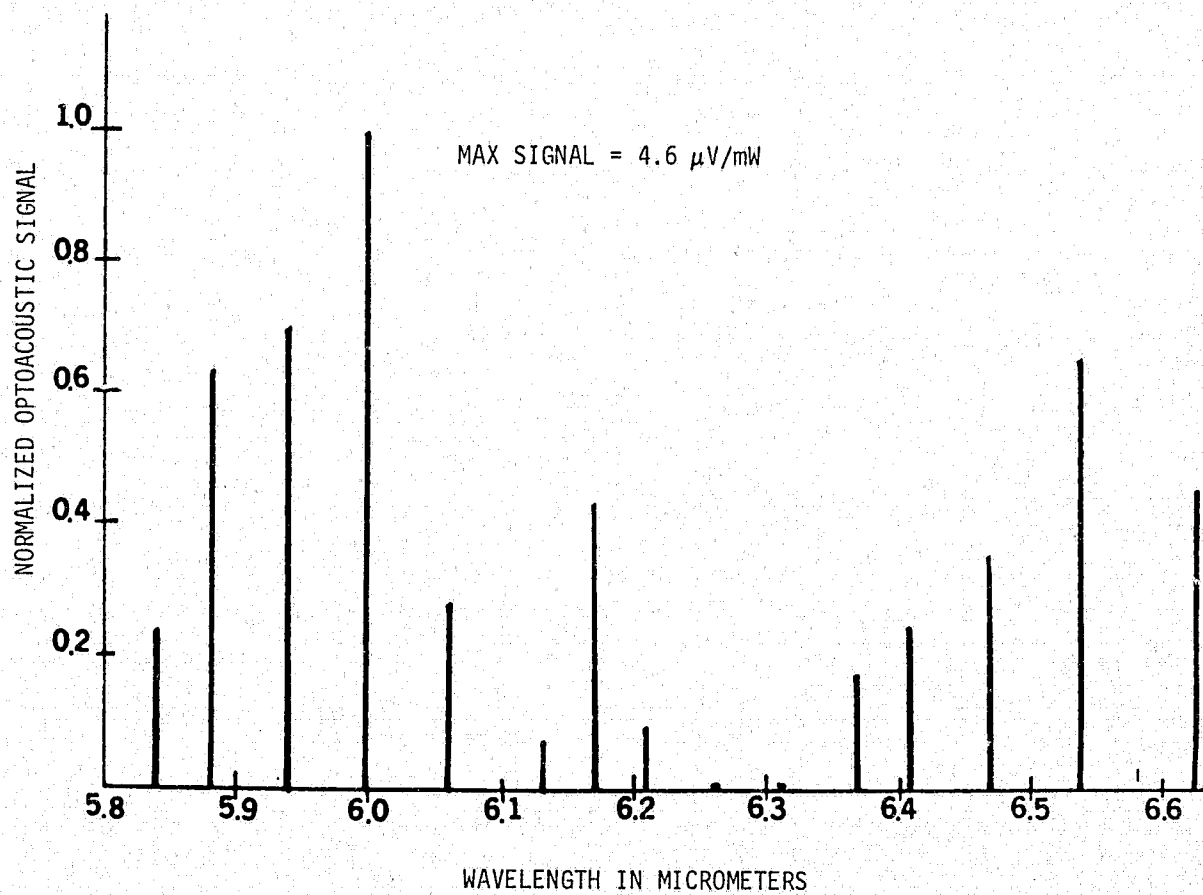


Figure B-3. Optoacoustic Spectrum of DNT at 6 Micrometers (45°C)

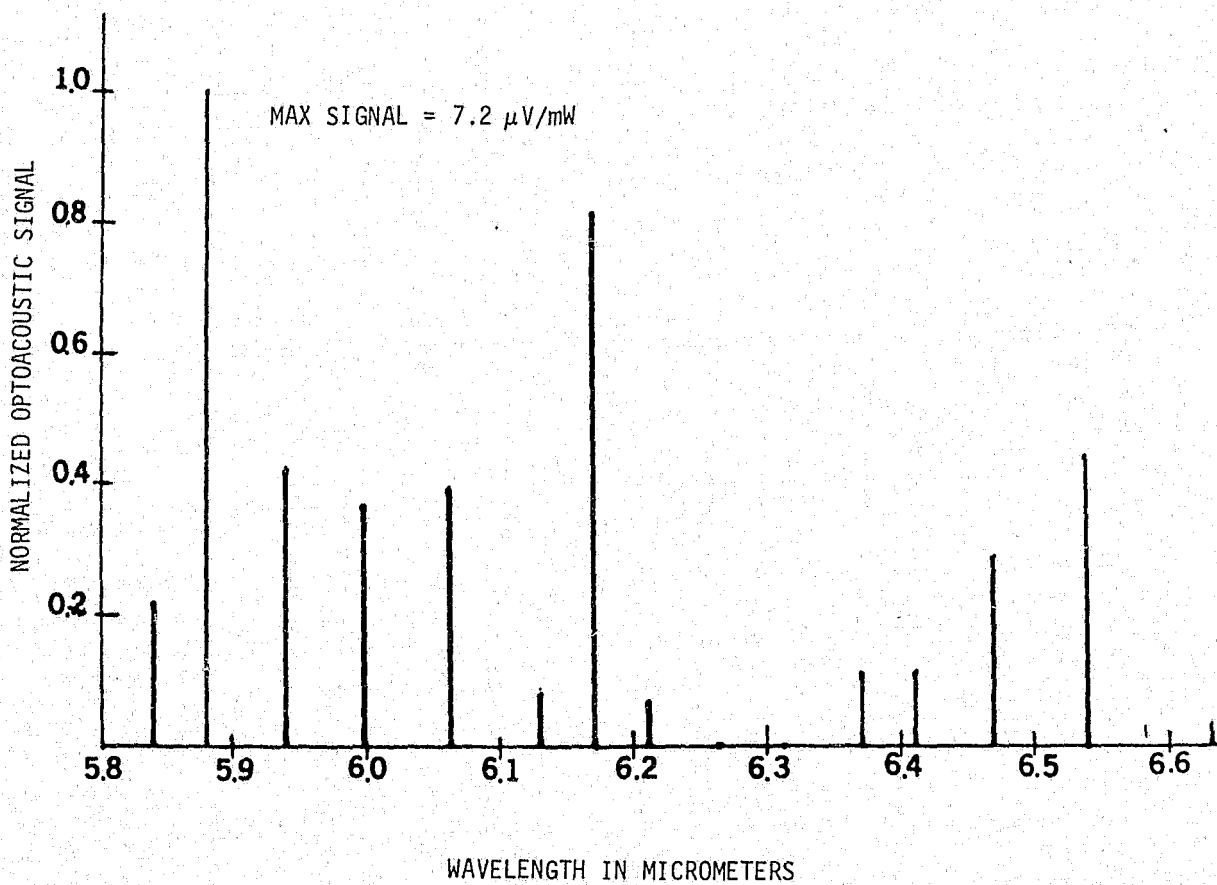


Figure B-4. Optoacoustic Spectrum of TNT at 6 Micrometers (45°C)
 (Spectrum is probably significantly contaminated with
 water vapor absorption spectrum)

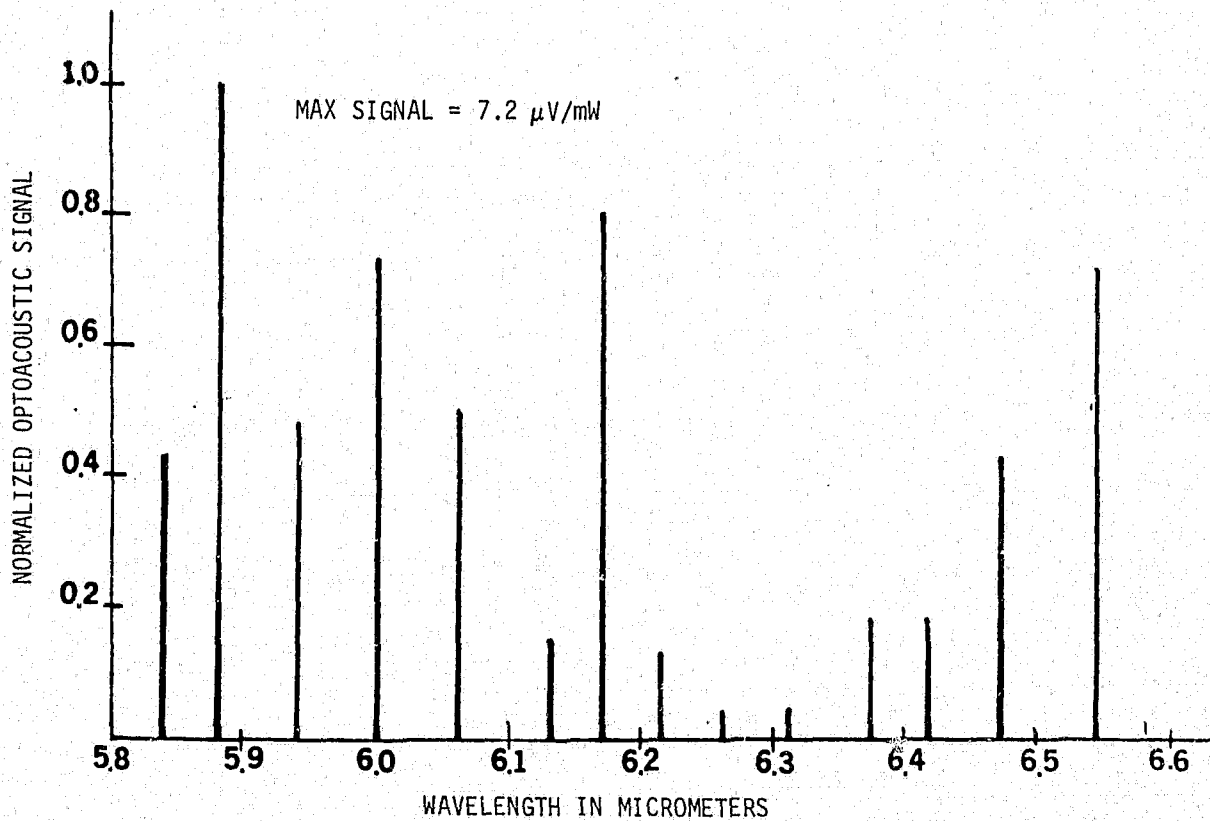


Figure B-5. Optoacoustic Spectrum of RDX at 6 Micrometers (45°C)
(Spectrum is probably significantly contaminated with
water vapor absorption spectrum)

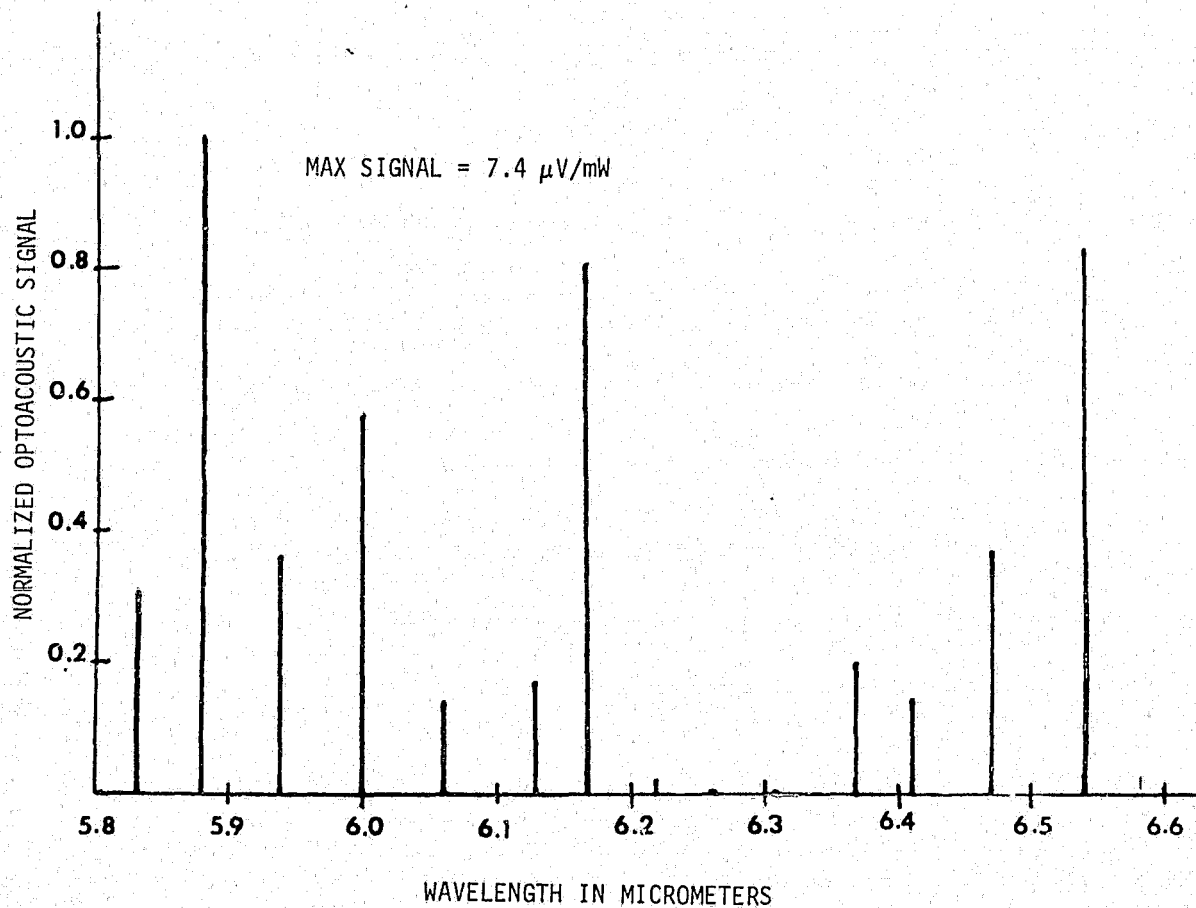


Figure B-6. Optoacoustic Spectrum of PETN at 6 Micrometers (45°C)
 (Spectrum is probably significantly contaminated with
 water vapor spectrum)

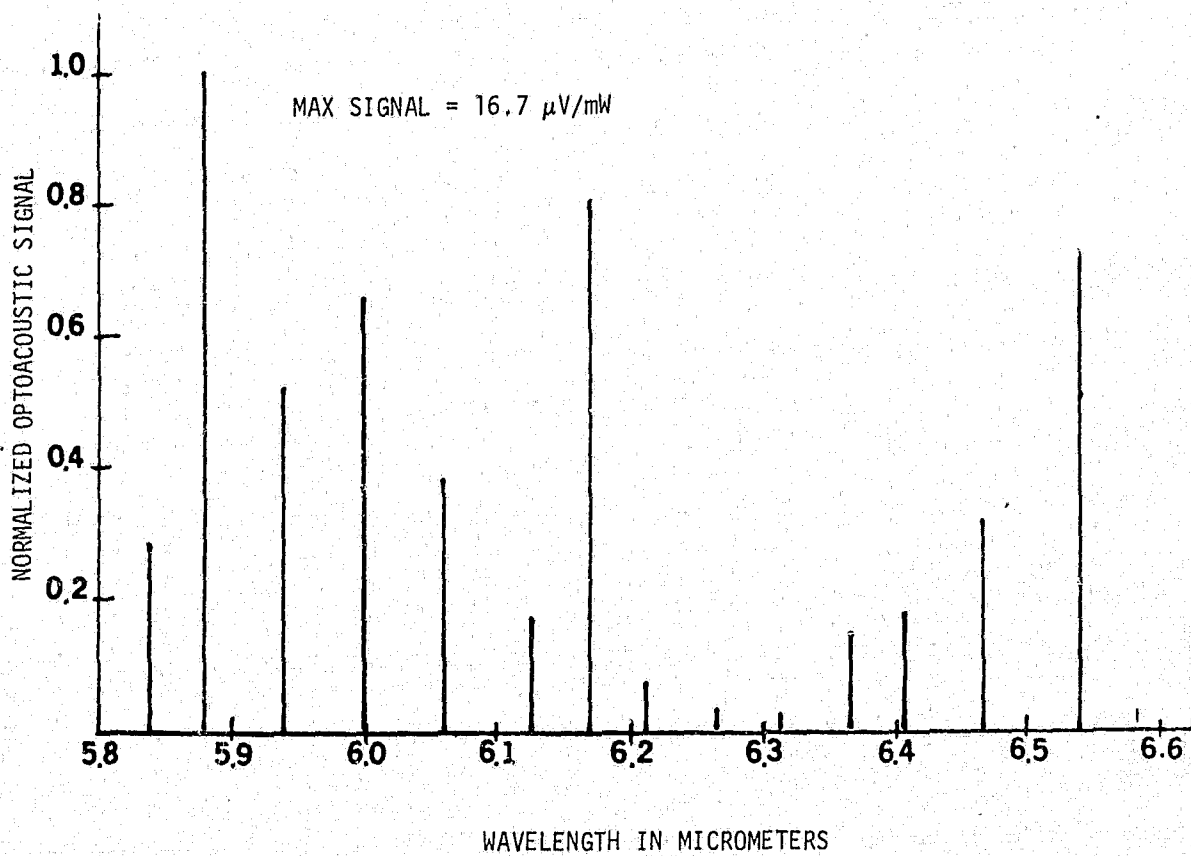


Figure B-7. Optoacoustic Spectrum of TOVEX at 6 Micrometers (45°C) (Spectrum is probably significantly contaminated with water vapor spectrum)

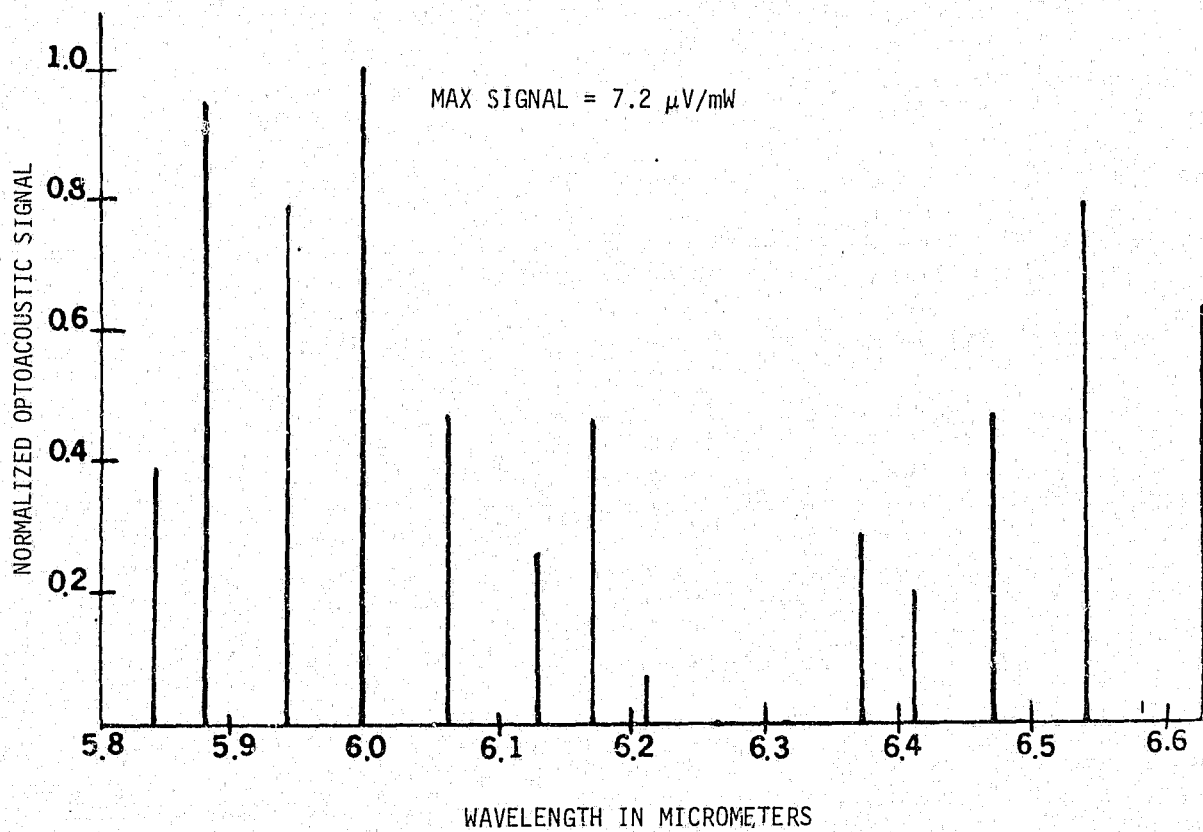


Figure B-8. Optoacoustic Spectrum of Dynamite at 6 Micrometers (45°C)

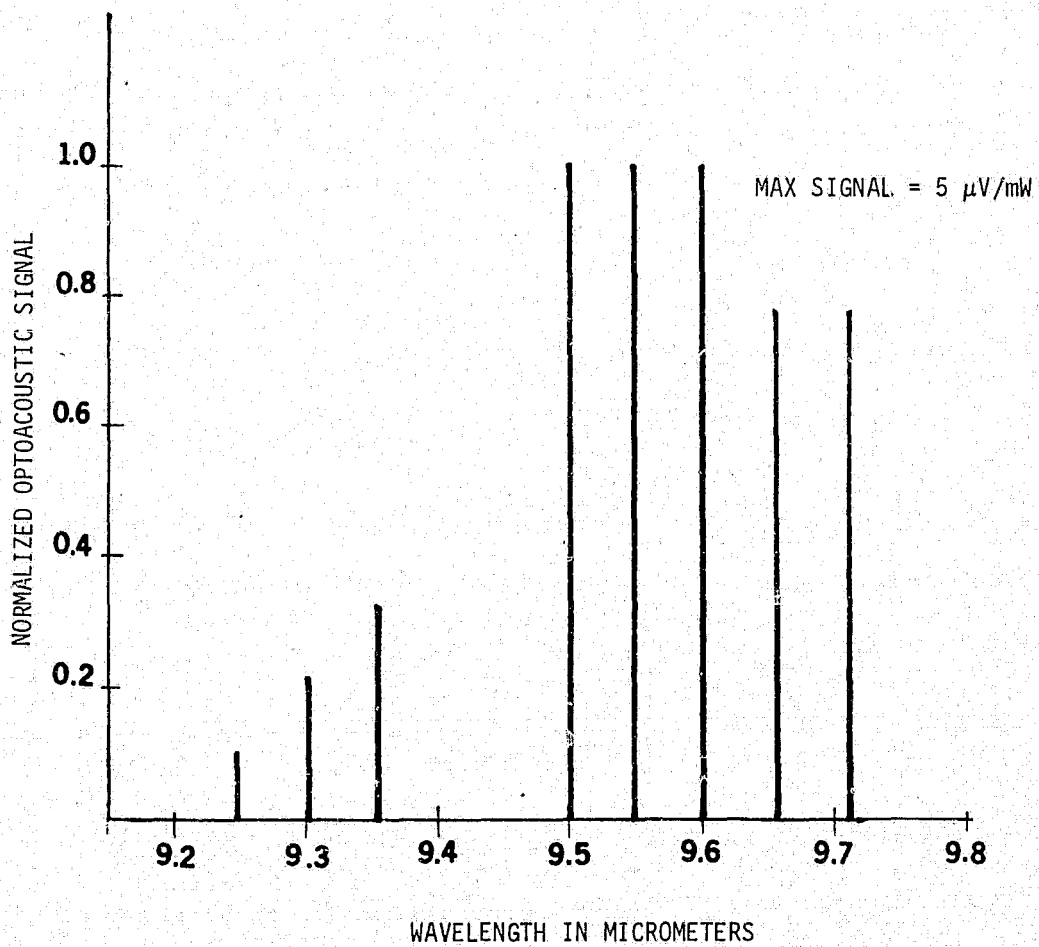


Figure B-9. Optoacoustic Spectrum of NG at 9 Micrometers (45°C)

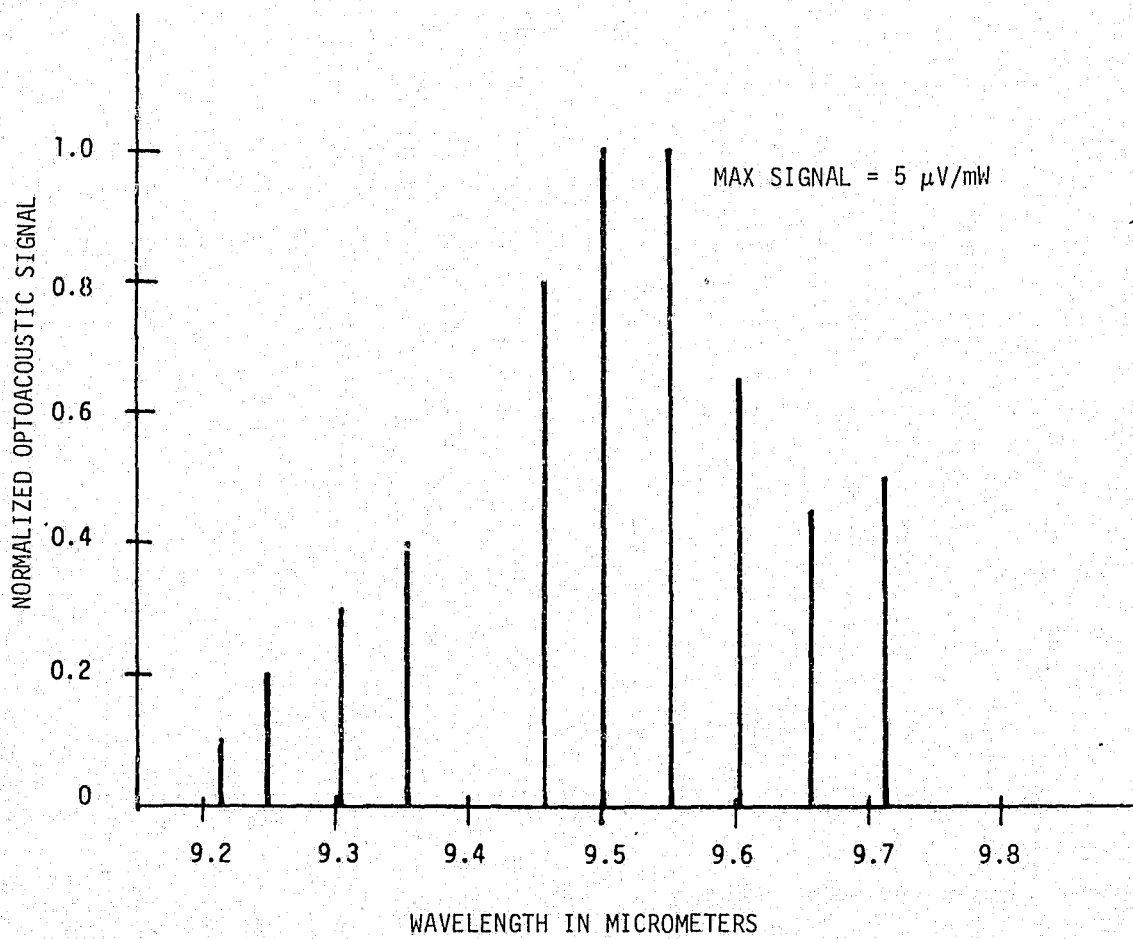


Figure B-10. Optoacoustic Spectrum of EGDN at 9 Micrometers (45°C)

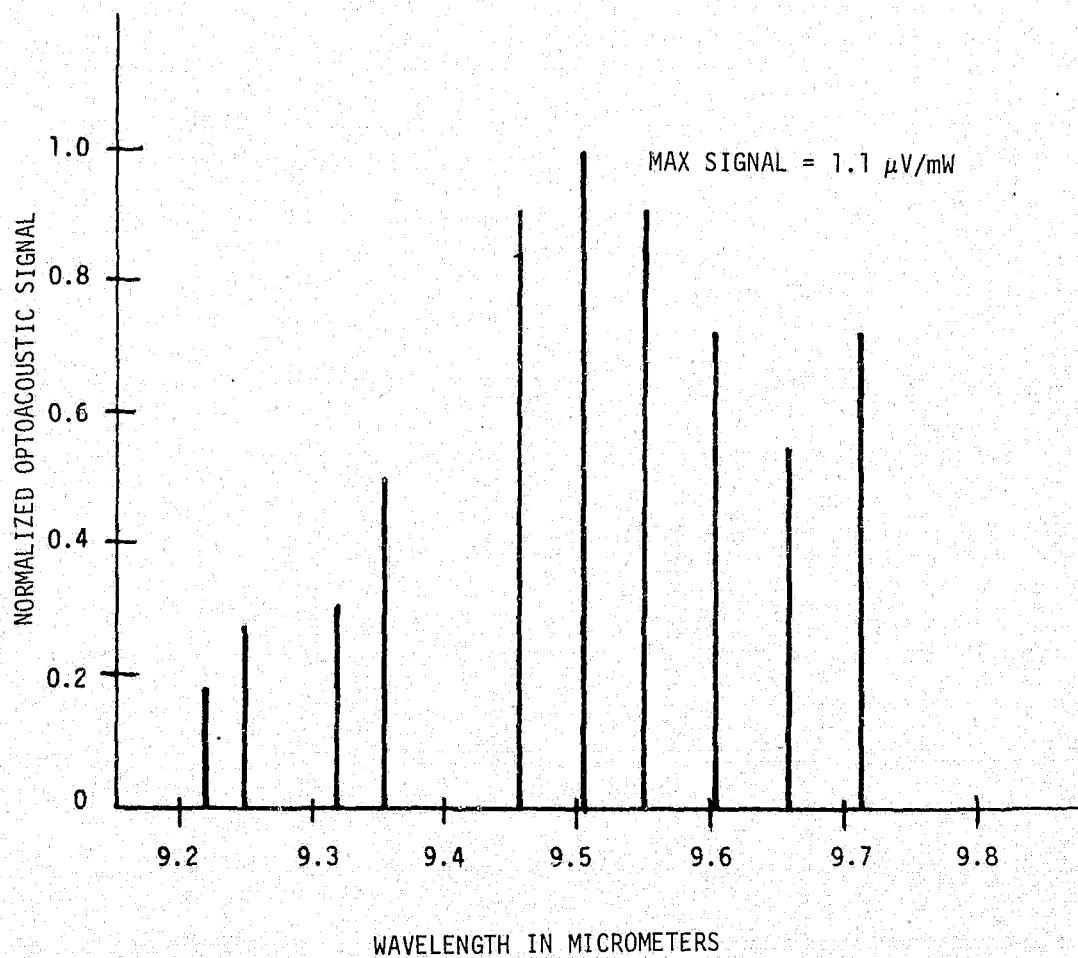


Figure B-11. Optoacoustic Spectrum of DNT at 9 Micrometers (45°C)

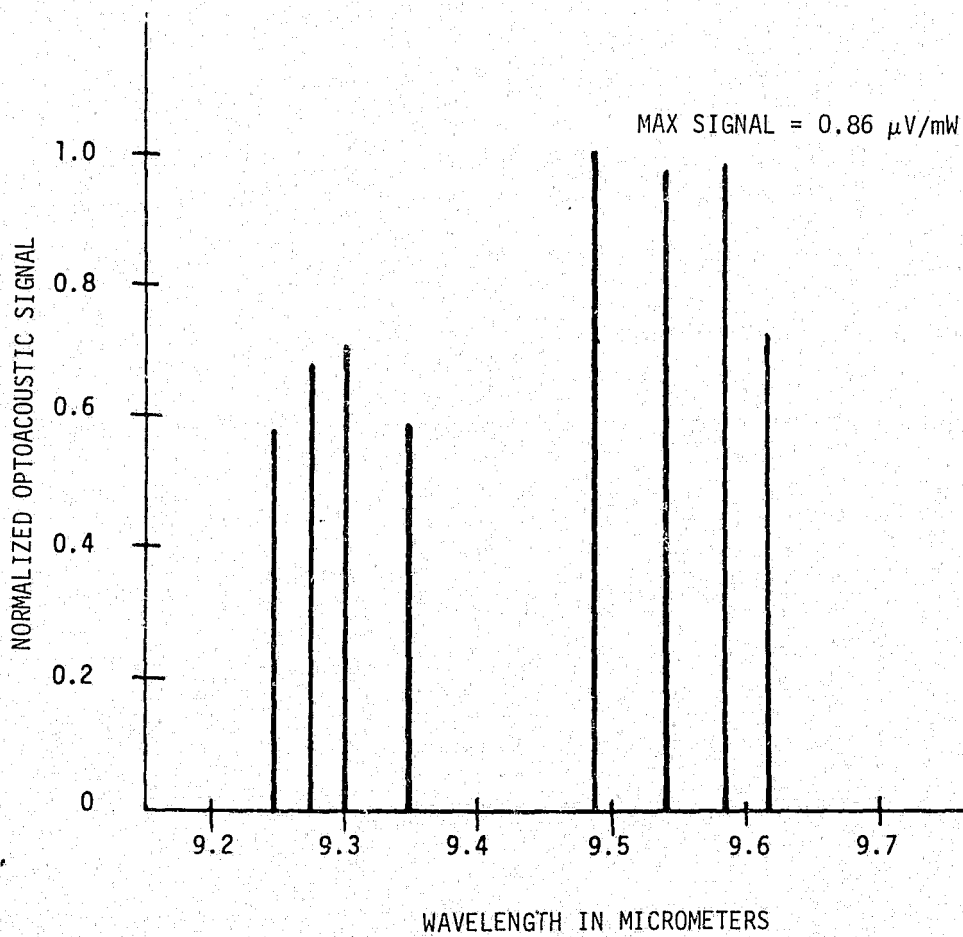


Figure B-12. Optoacoustic Spectrum of Dynamite at 9 Micrometers (45°C)

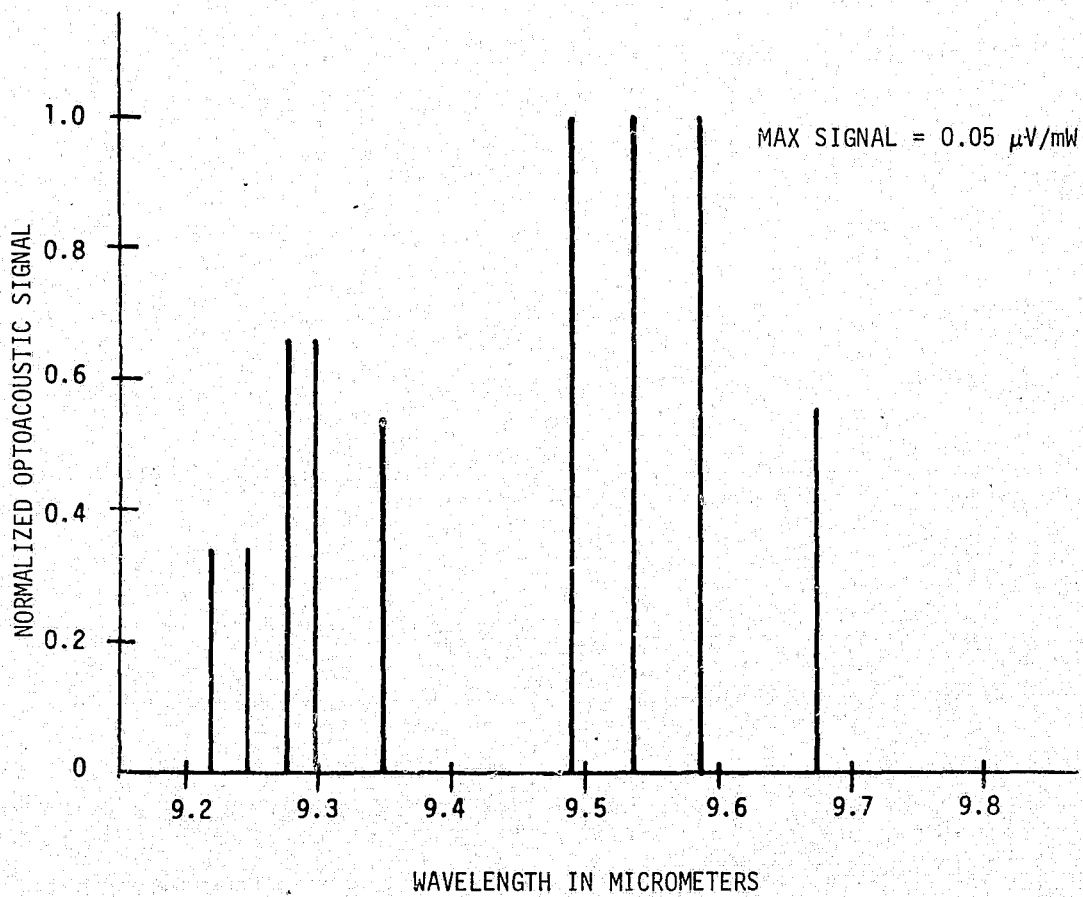


Figure B-13. Optoacoustic Spectrum of Black Powder at 9 Micrometers (45°C)

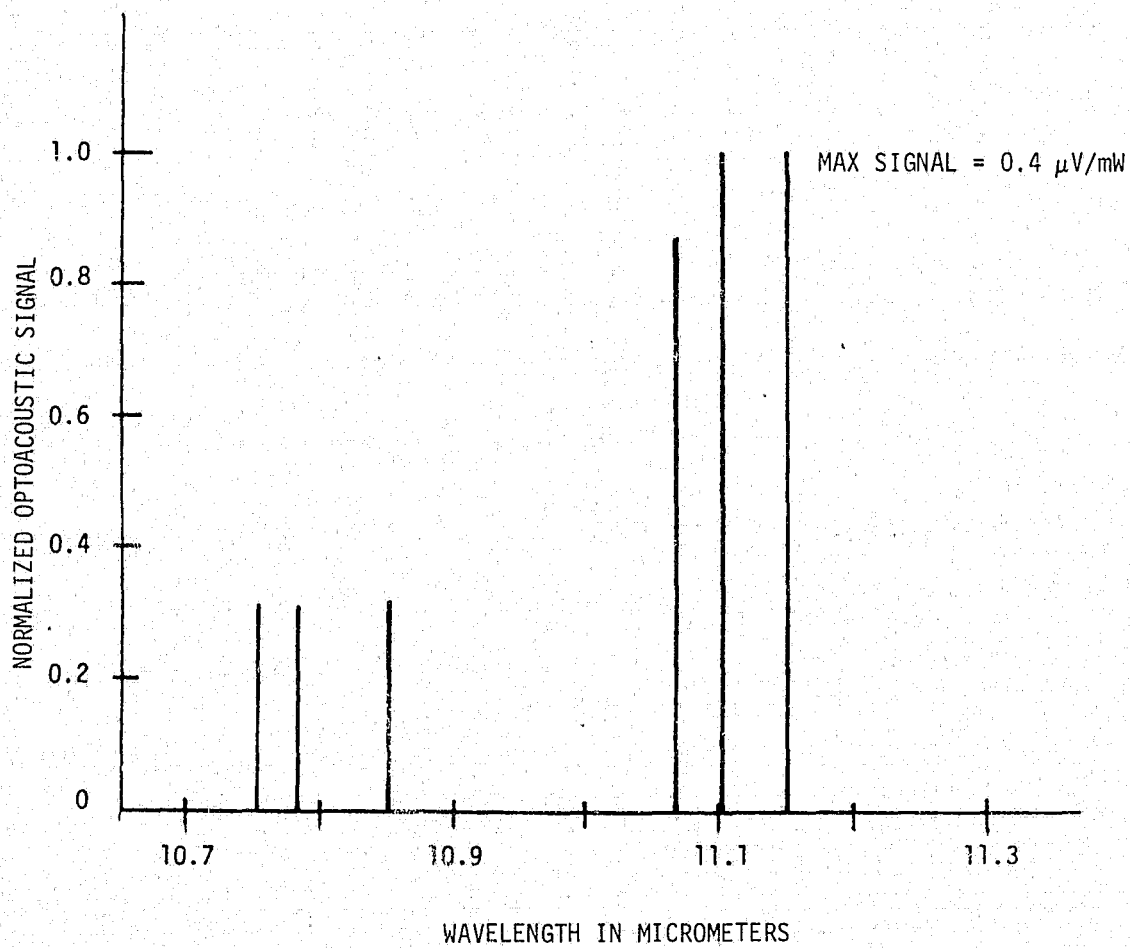


Figure B-14. Optoacoustic Spectrum of NG at 11 Micrometers (23°C)

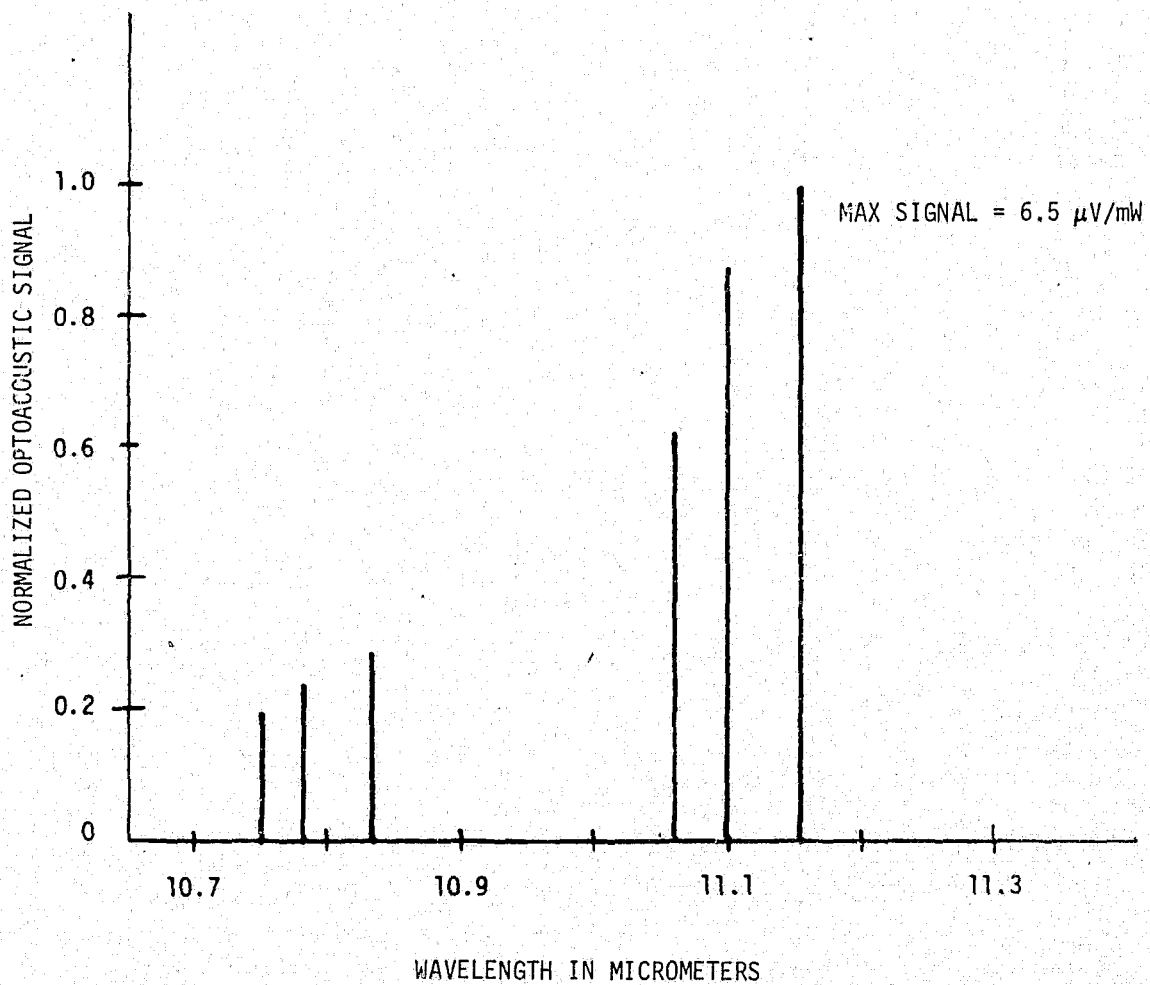


Figure B-15. Optoacoustic Spectrum of NG at 11 Micrometers (45°C)

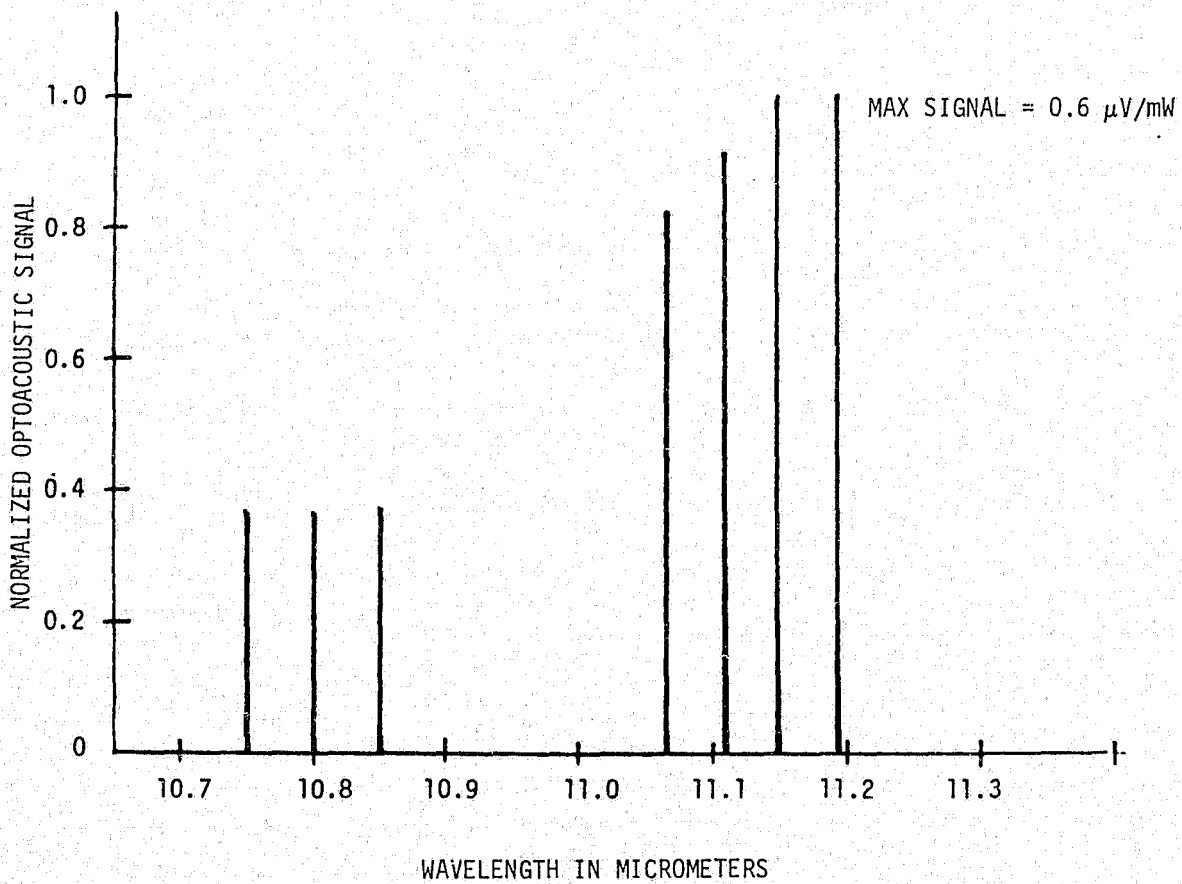


Figure B-16. Optoacoustic Spectrum of EGDN at 11 Micrometers (23°C)

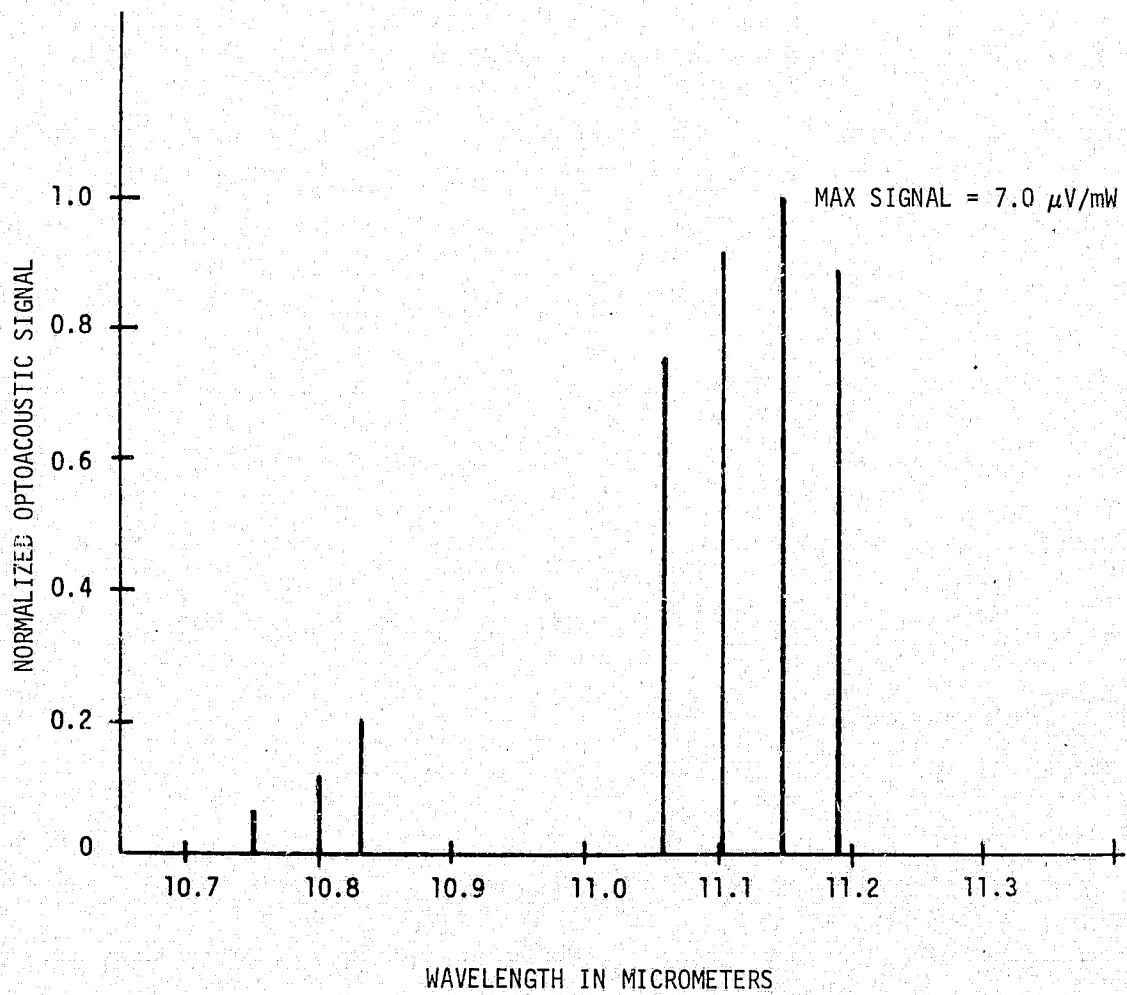


Figure B-17. Optoacoustic Spectrum of EGDN at 11 Micrometers (45°)

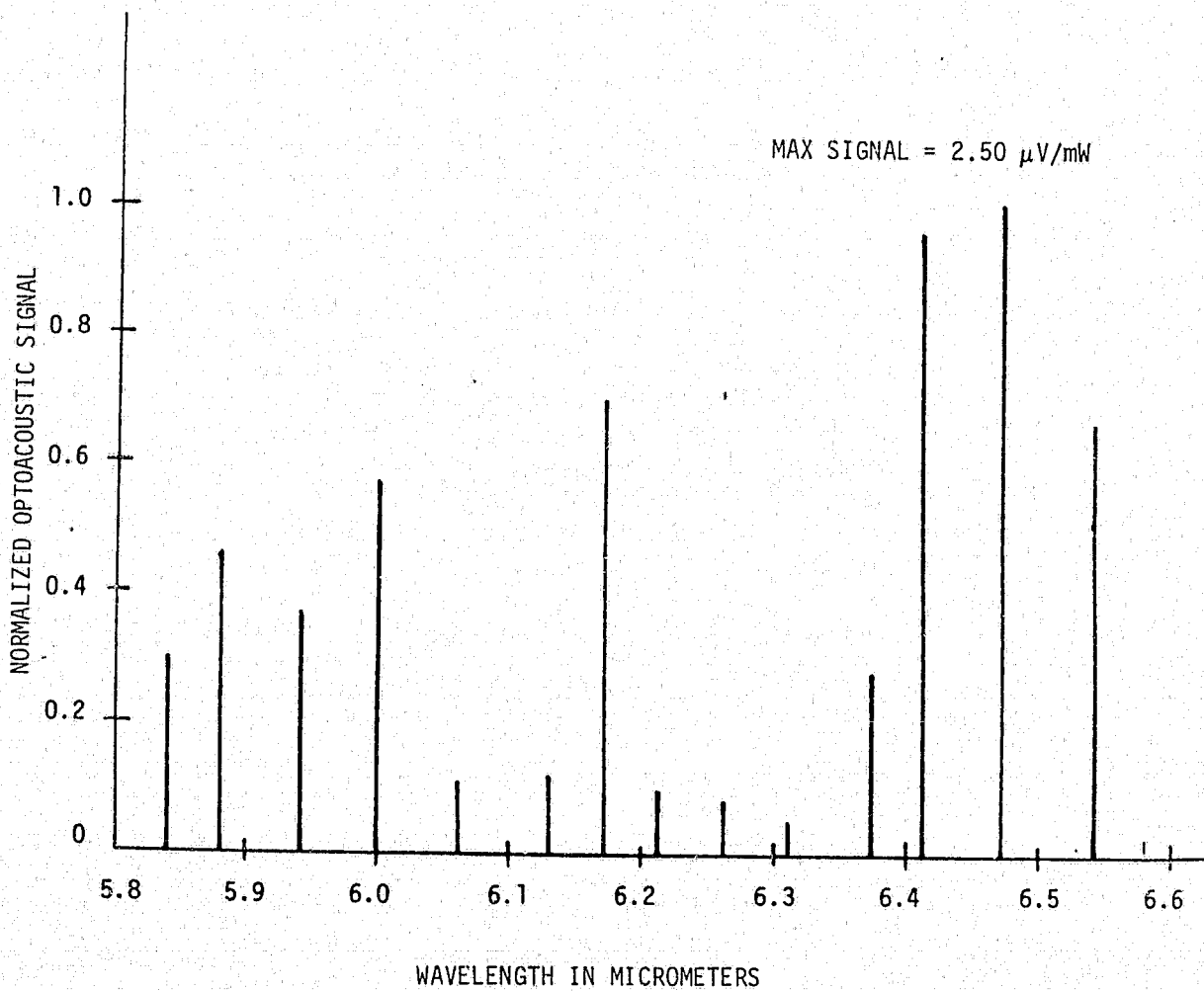


Figure B-18. Optoacoustic Spectrum of Butane at 6 Micrometers

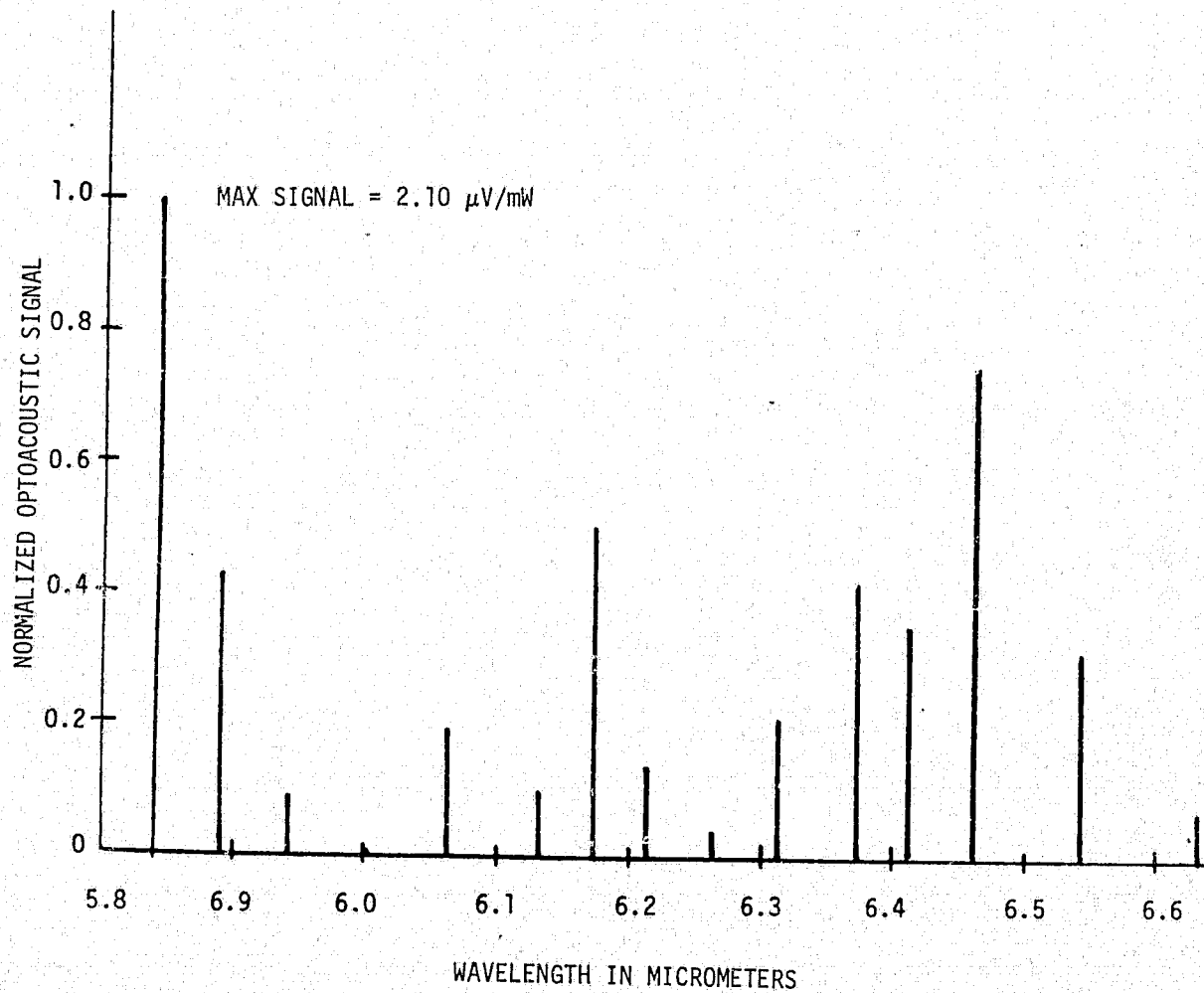


Figure B-19. Optoacoustic Spectrum of Methane at 6 Micrometers

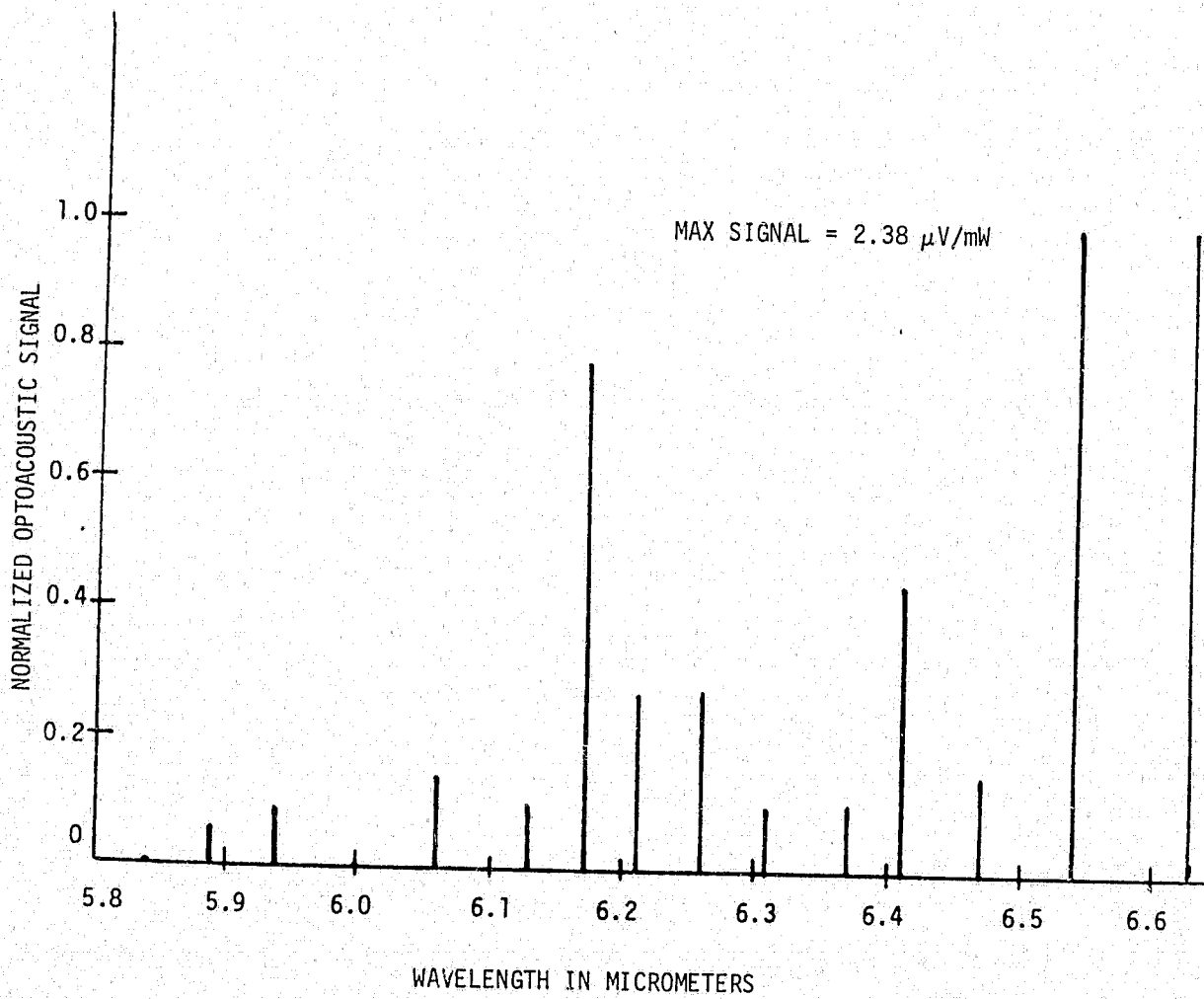


Figure B-20. Optoacoustic Spectrum of NO at 6 Micrometers

CONTINUED

1 OF 2

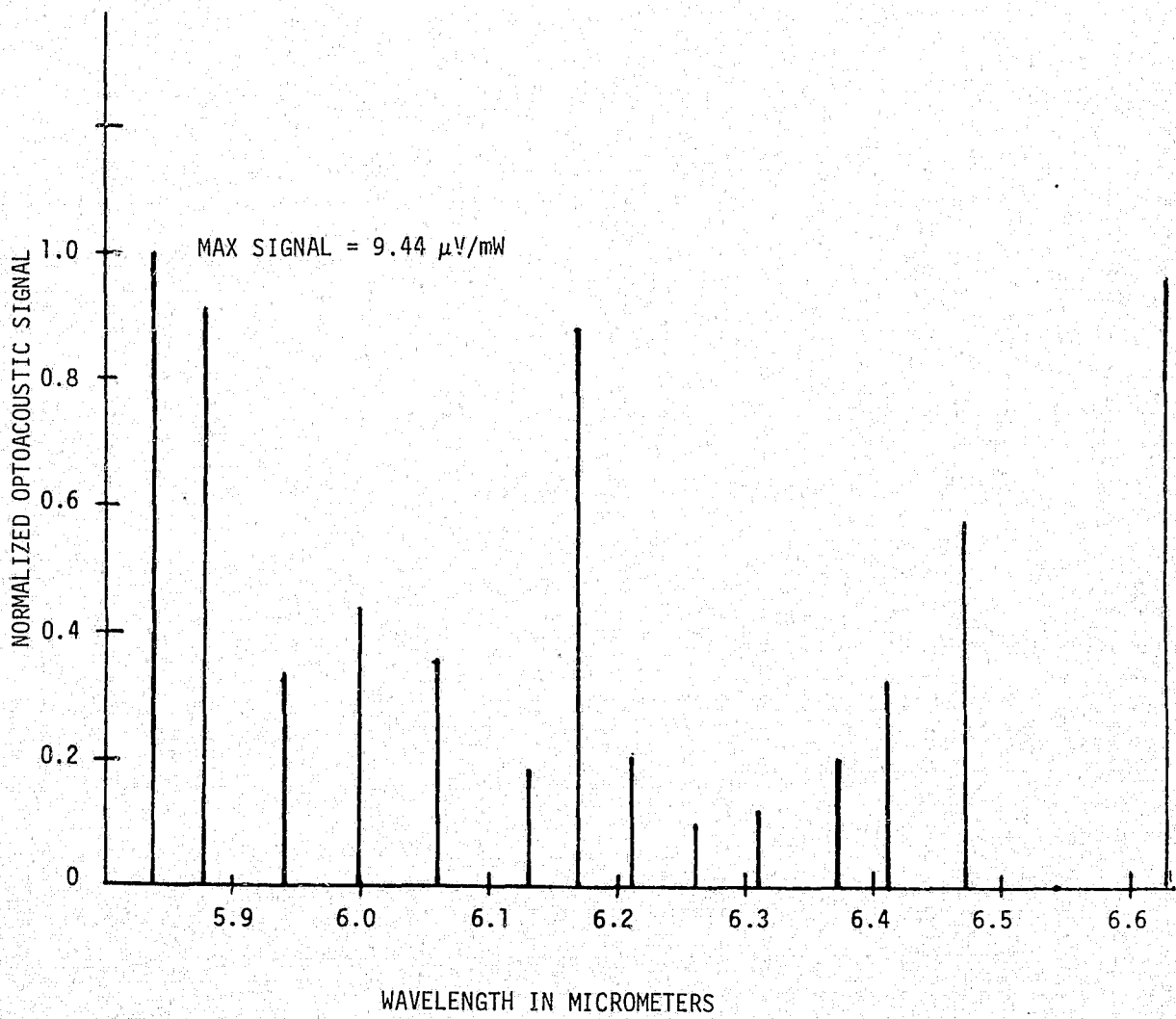


Figure B-21. Optoacoustic Signal of NO_2 at 6 Micrometers

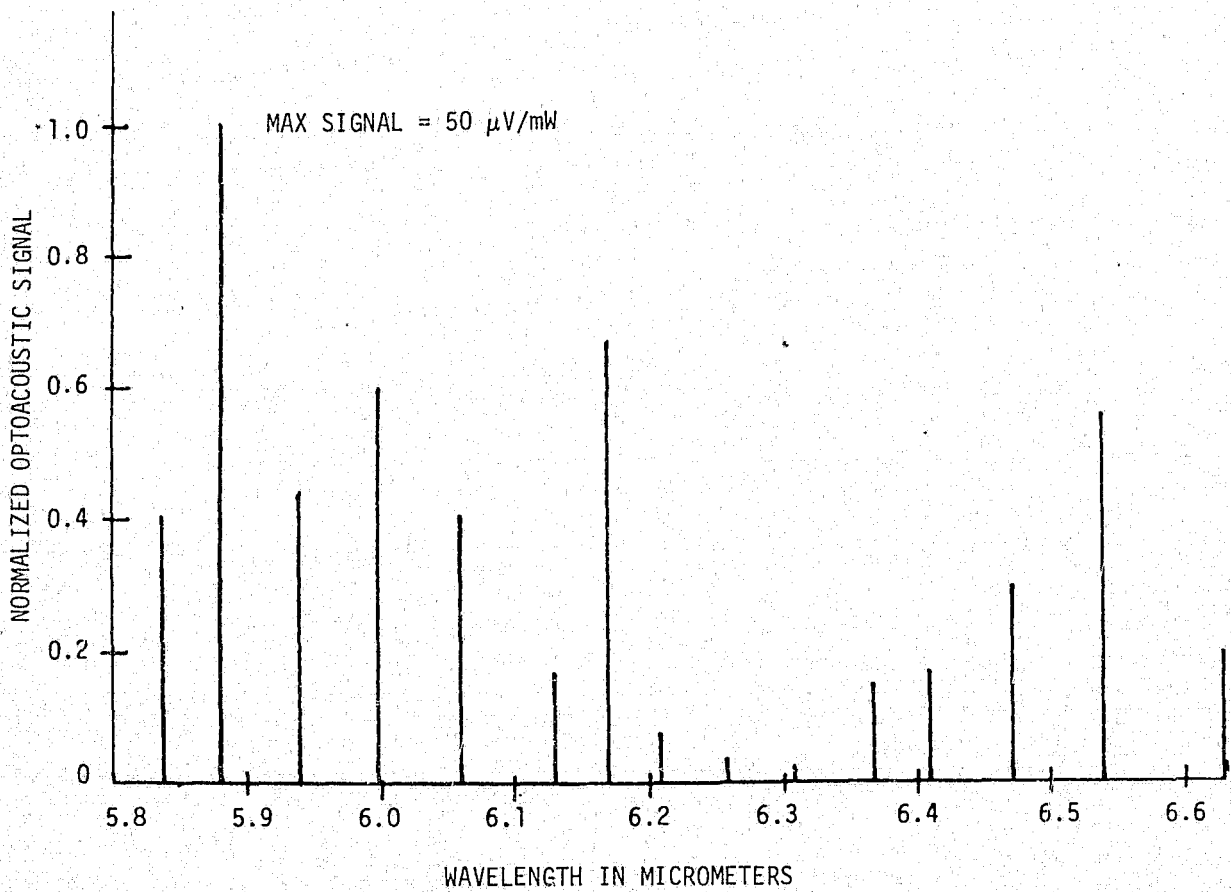


Figure B-22. Optoacoustic Spectrum of Water Vapor at 6 Micrometers

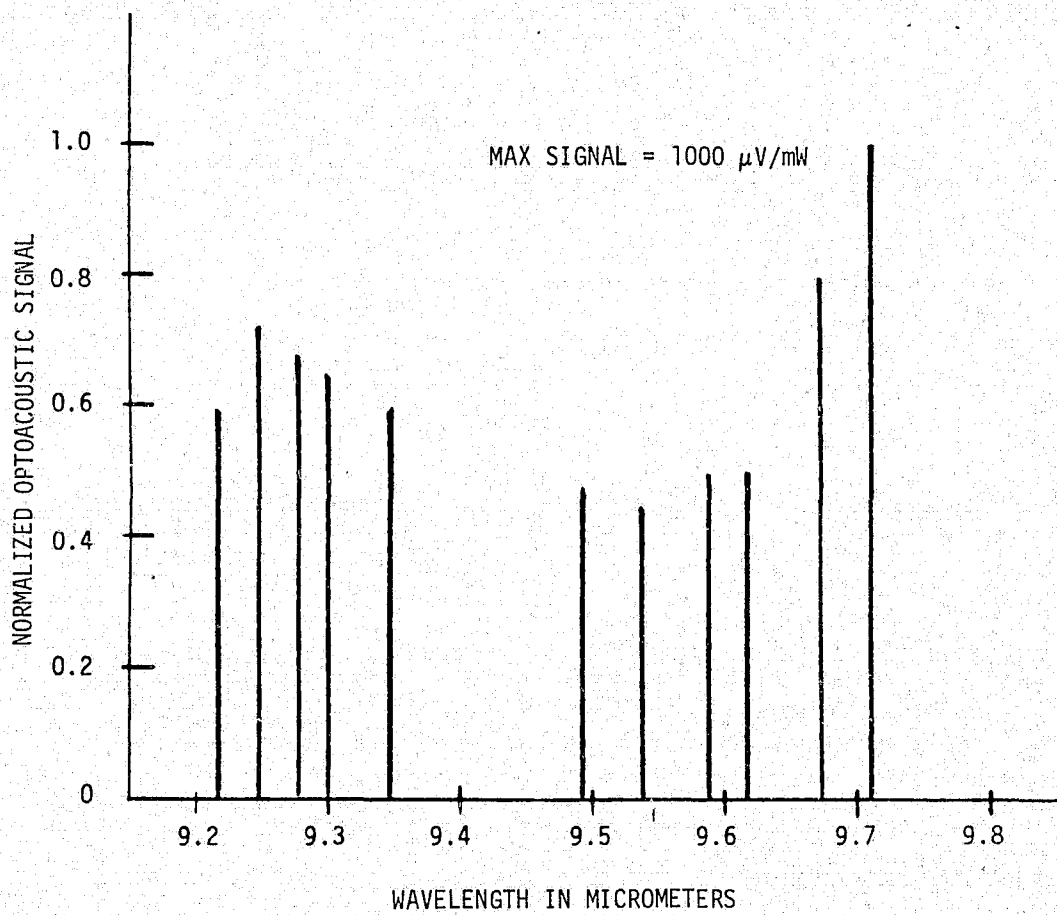


Figure B-23. Optoacoustic Spectrum of Butane at 9 Micrometers

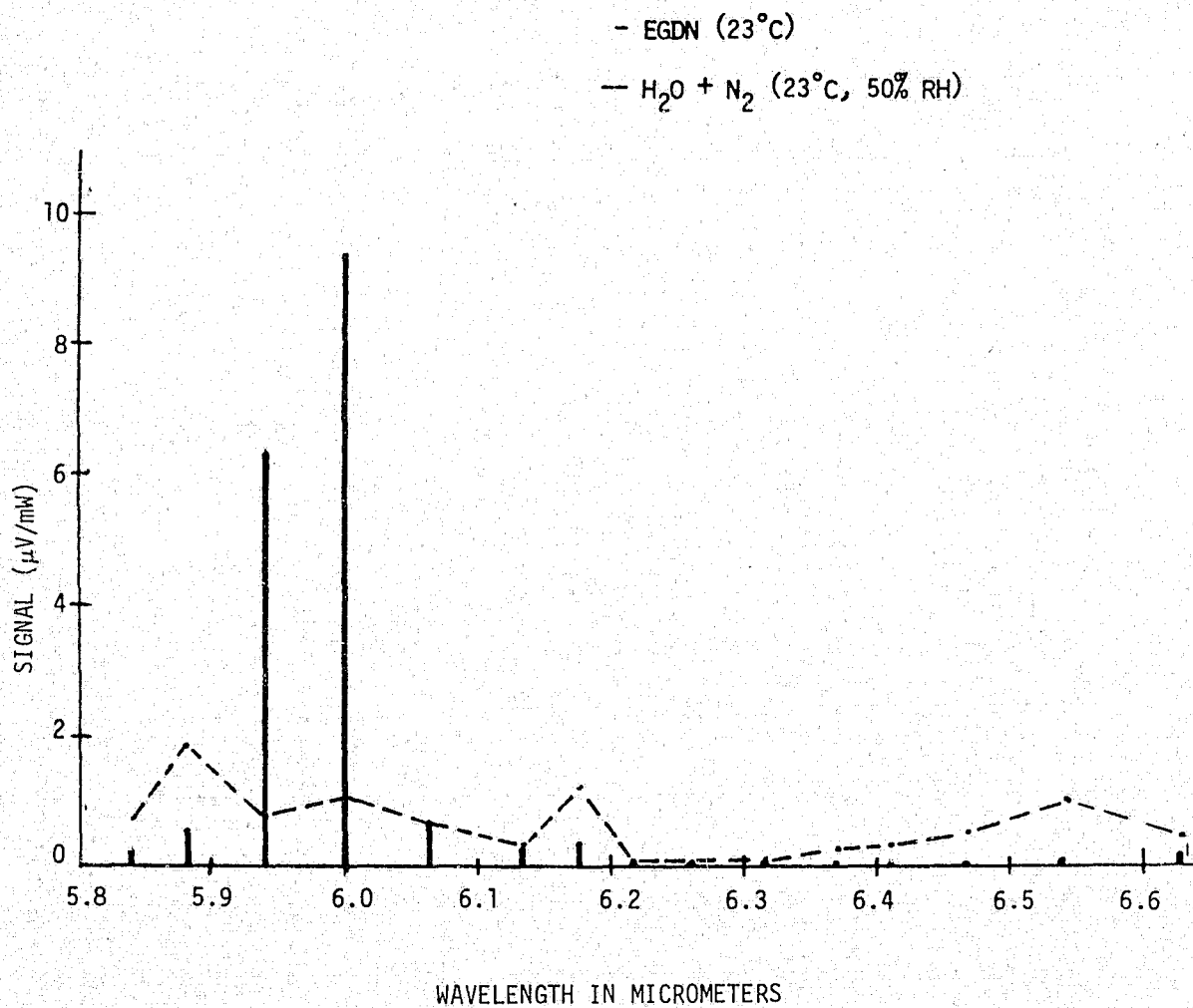


Figure B-24. Comparison of EGDN and Water Vapor Optoacoustic Spectra at 6 Micrometers (50% Relative Humidity)

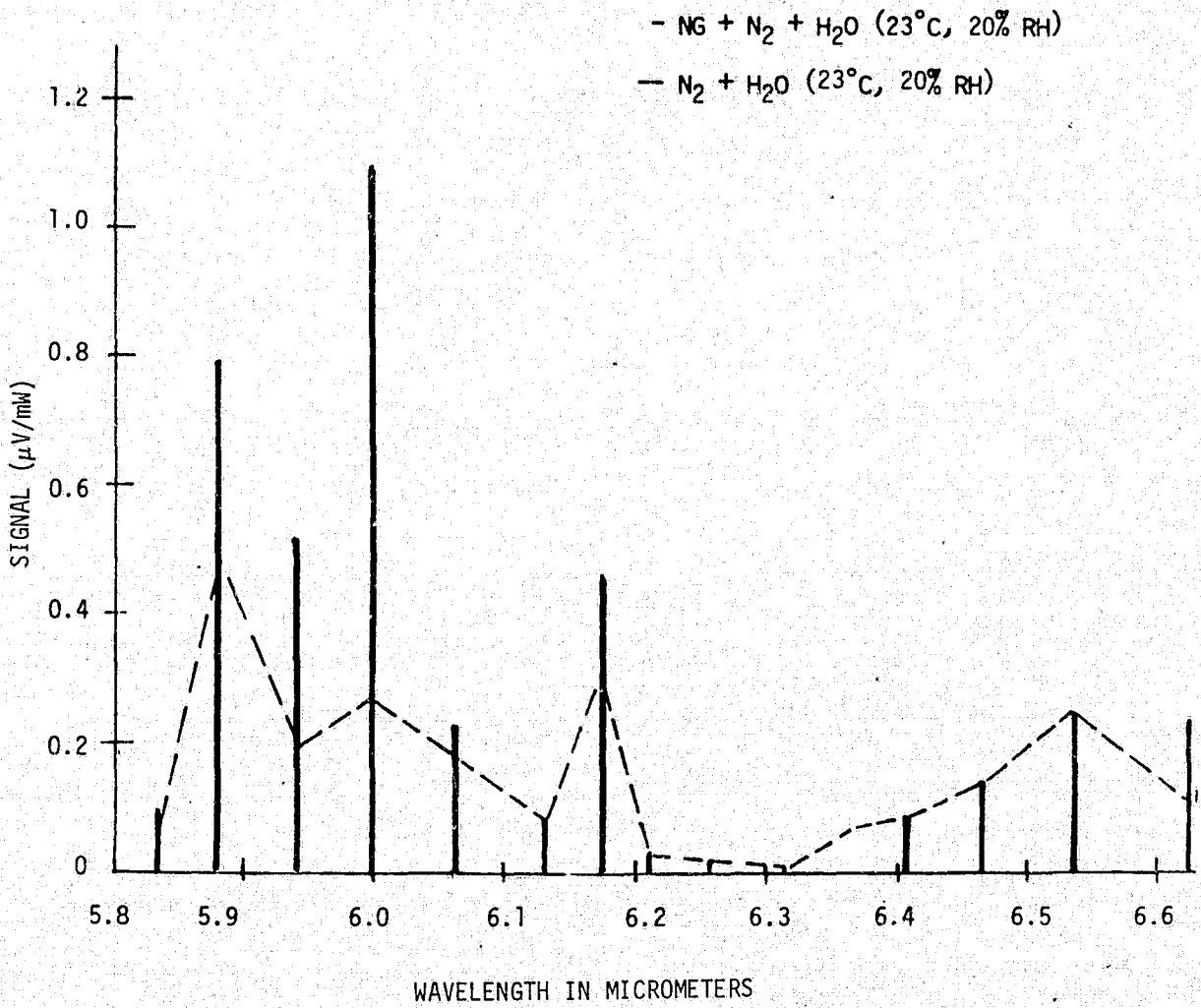


Figure B-25. Comparison of NG and Water Vapor Optoacoustic Spectra at 6 Micrometers (20% Relative Humidity)

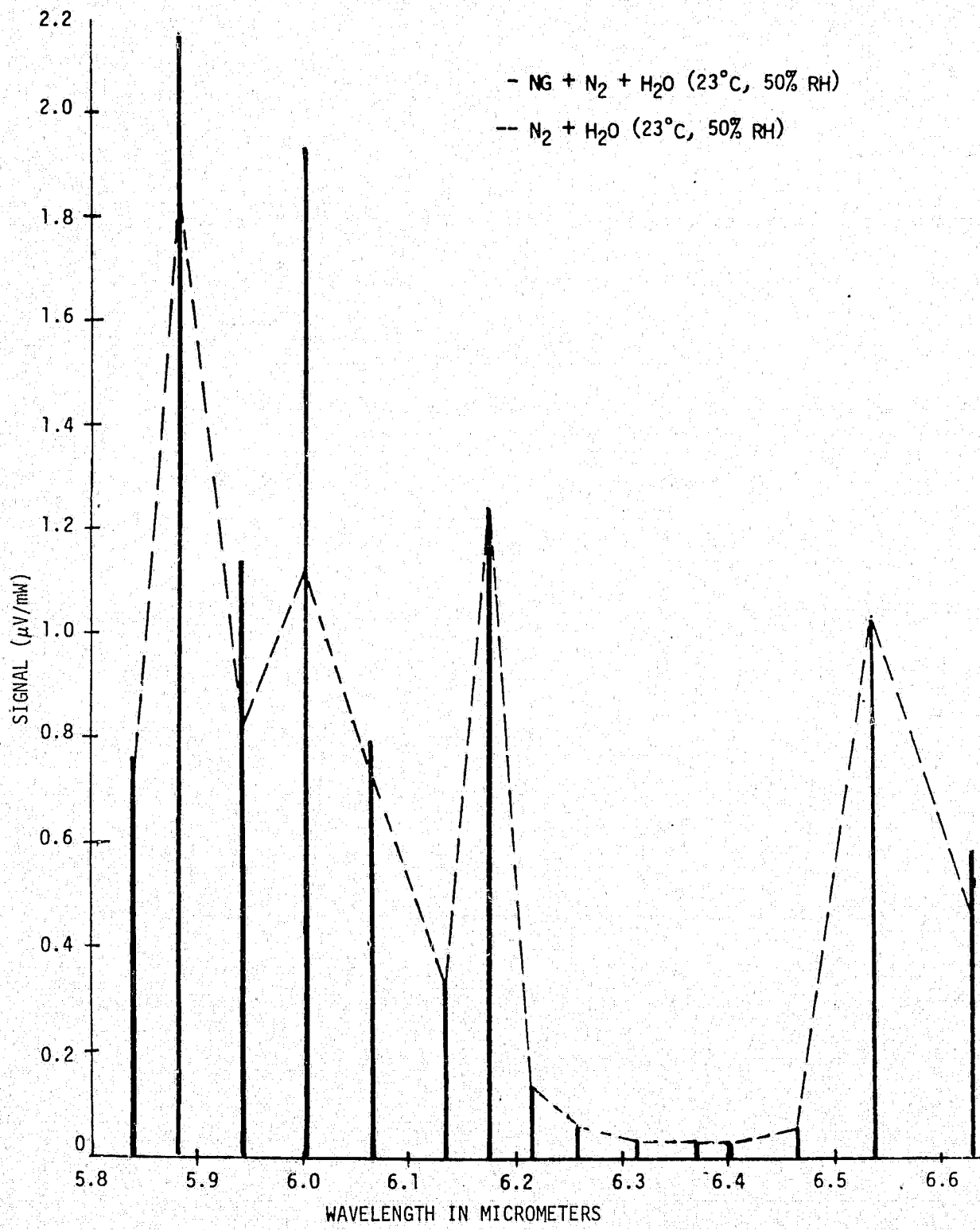


Figure B-26. Comparison of NG and Water Vapor Optoacoustic Spectra at 6 Micrometers (50% Relative Humidity)

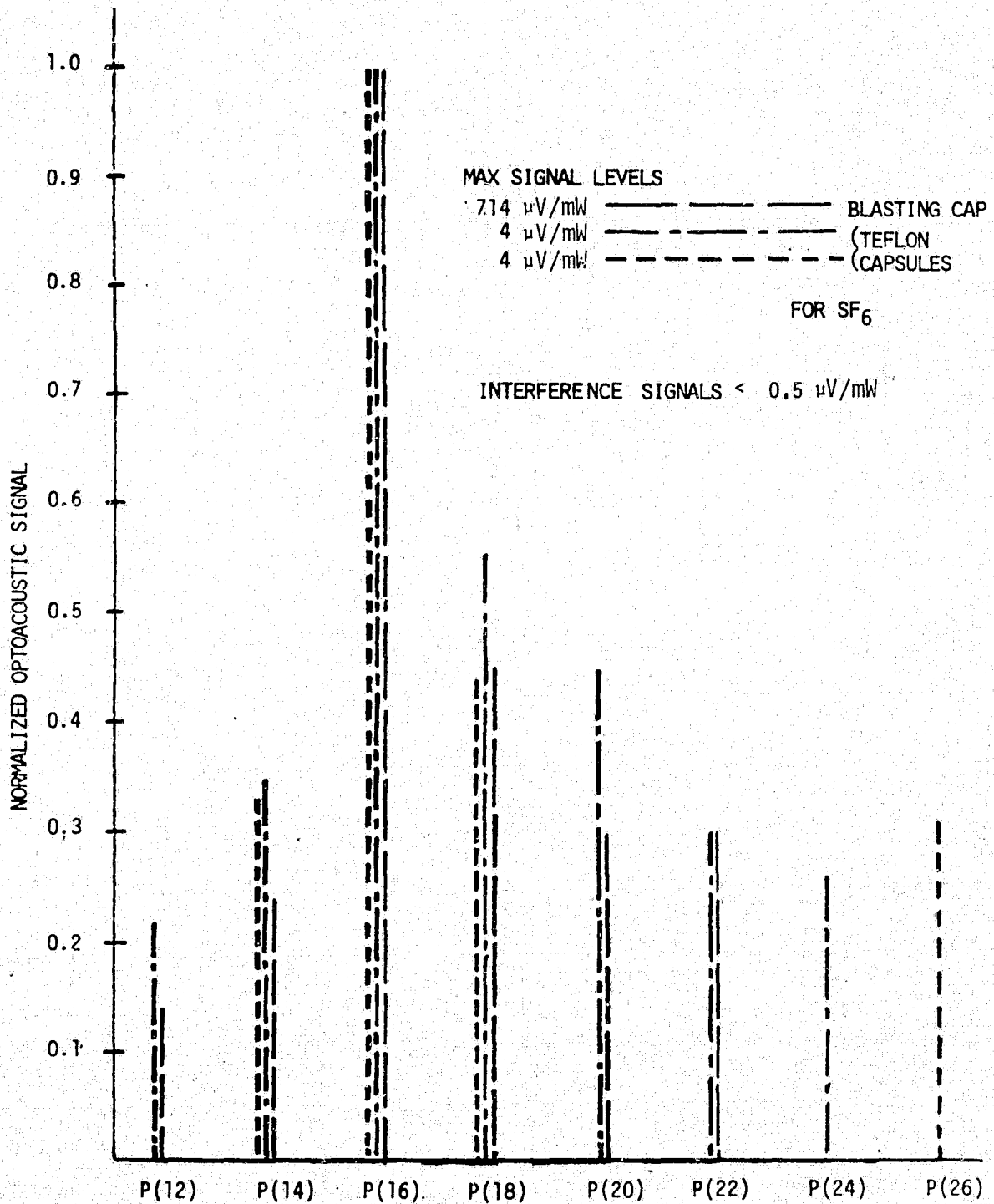


Figure B-27. Optoacoustic Detection of SF₆ in the 10.6 Micrometer Wavelength Region

NOTES

1. Yusek, R., "CO Laser Frequency Stabilization Using Resonant Absorption in SF", Ph.D. Dissertation, Case Western Reserve University, (1970).
2. Rakaczky, J. A. and A. D. Coates, The Effect of Surfaces on the Flow of Vaporized Explosives, Ballistics Research Laboratory, Aberdeen Proving Ground, Md., BRL Report No. 1597.
3. Urbanski, Tadeusz, Chemistry and Technology of Explosives, Pergamon Press, (1964).
4. Coates, A. D., Eli Freeman, Lester P. Kuhn, Characteristics of Certain Military Explosives, Ballistics Research Laboratory, Aberdeen Proving Ground, Md. BRL Report No. 1507, (Nov. 1970).
5. Pristera, F., M. Halik, A. Castelli, and W. Fredericks, "Analysis of Explosives Using Infrared Spectroscopy", Anal. Chem. Vol. 32, pp. 495-508, (April 1960).
6. Standard IR Spectra, Sadtler Research Laboratories, Inc., Philadelphia, Pa.
7. Shaw, J. H., "Nitric Oxide Fundamental", J. Chem. Phys., Vol. 24, pp. 399-402 (Feb. 1956).
8. Hurlock, S. C., K. N. Rao, L. A. Weller, and P. K. L. Yin, "High Resolution Spectrum and Analysis of the ν_2 Band of $^{14}\text{N}^{16}\text{O}_2$ ", J. Mol. Spectrosc., Vol. 48, pp. 372-394 (Nov. 1973).

END